



RÉPUBLIQUE ALGÉRIENNE DÉMOCRATIQUE ET POPULAIRE
MINISTÈRE DE L'ENSEIGNEMENT SUPÉRIEUR ET DE LA RECHERCHE SCIENTIFIQUE
UNIVERSITÉ MOHAMED BOUDIAF - M'SILA
FACULTÉ DE MATHÉMATIQUES ET DE L'INFORMATIQUE
DÉPARTEMENT DE MATHÉMATIQUES



N° d'ordre :

THÈSE

*Présentée pour l'obtention du diplôme
de Doctorat en sciences*

Spécialité

Mathématiques

Option

Mathématiques appliquées

Par

Tahar Blizak

Thème

**Traitement numérique d'un problème d'écoulement
bidimensionnel de type jet devant un objet
rectangulaire**

Soutenue le 05/10/2023 devant le jury composé de :

Brahim BOUDERAH	Prof	Université de M'sila	Président
Abdelkader GASMI	Prof	Université de M'sila	Directeur
Abdelkrim MERZOUGUI	Prof	Université de M'sila	Examineur
Abdelkader LAIADI	MCA	Université de Biskra	Examineur
Abdelkader AMARA	MCA	Université de Ouargla	Examineur
Brahim TELLAB	MCA	Université de Ouargla	Examineur

Msila University

Faculty of Mathematics and Informatics

Numerical treatment of a problem two-
Dimensional Fluid Flow Past a Rectangular
object

BLIZAK TAHAR

Thesis submitted in fulfillment of the
requirements

for the degree of

Doctorate of Science in Mathematics

Academic year 2023-2024

acknowledgments

Alhamdulillah, I am grateful to Allah who enabled me to complete this work. Without Him, nothing would have been achieved. I thank Him and praise Him for His grace.

I would like to express my deepest gratitude to my supervisor, Prof. Gasmi Abdelkader, for providing me with knowledge, motivation, and constant support that kept me motivated to complete this thesis.

I sincerely thank the chairman of the jury committee, Prof. Brahim Bouderah, and the other jury members, Prof. Abdelkrim Merzougui, Dr. Abdelkader Laiadi, Dr. Abdelkader Amara, and Dr. Tellab Brahim for agreeing to read the manuscript.

A big thank you to my colleagues in the Mathematics department for their help, encouragement, and warm welcome.

I am also grateful to all my friends. Finally, I would like to express my appreciation to my family for their support and encouragement. Each of them has helped me become who I am today, and without them, I would not have been able to write this thesis.

Abstract

In this thesis, we investigate two problems in the field of fluid dynamics:

1. The first problem involves the impact of an infinite wedge on a jet at a considerable distance. In this case, we employed the Hodograph method to obtain analytical solutions. Subsequently, we numerically solved the problem using the boundary integral equation technique, taking into account the influence of surface tension.
2. The second problem deals with the effect of a finite wedge positioned inside an infinite straight channel on the flow of a fluid. For this problem, we used series truncation methods to address and solve it.

Keywords : Potential flow, incompressible fluid, free surface, surface tension, Weber number, conformal transformation, truncation of the series, boundary integral equation technique.

المخلص

في هذه الأطروحة، قمنا بدراسة مشكلتين في مجال ديناميكا الموائع:
1. المشكلة الأولى تتعلق بتأثير إسفين لا نهائي على تدفق نفاث على مسافة كبيرة. في هذه الحالة، استخدمنا طريقة الجسم للحصول على الحلول التحليلية. وبعد ذلك، قمنا بحل المشكلة عددياً باستخدام تقنية المعادلة التكاملية الحدودية، مع الأخذ بعين الاعتبار تأثير التوتر السطحي.
2. المشكلة الثانية تتعلق بتأثير الإسفين المحدود الموجود داخل قناة مستقيمة لا نهائية على تدفق السائل. بالنسبة لهذه المشكلة، استخدمنا طرق اقتطاع السلسلة لمعالجتها وحلها.
الكلمات المفتاحية: التدفق، السائل غير القابل للضغط، السطح الحر، التوتر السطحي، رقم ويبر، التحويل المحافظ، اقتطاع السلسلة، تقنية المعادلة الحدودية التكاملية.

Résumé

Dans cette thèse, nous étudions deux problèmes dans le domaine de la dynamique des fluides :

1. Le premier problème concerne l'impact d'un coin infini sur un jet à une distance considérable. Dans ce cas, nous avons utilisé la méthode de Hodographe pour obtenir des solutions analytiques. Par la suite, nous avons résolu numériquement le problème en utilisant la technique de l'équation intégrale aux limites, en tenant compte de l'influence de la tension superficielle.
2. Le deuxième problème concerne l'effet d'un coin fini positionné à l'intérieur d'un canal droit infini sur l'écoulement d'un fluide. Pour ce problème, nous avons utilisé des méthodes de troncature en série pour le résoudre.

Mots clés : Ecoulement potentiel, fluide incompressible, surface libre, tension superficielle, nombre de Weber, transformation conforme, troncature de la série, technique d'équation intégrale aux limites.

Contents

acknowledgments	i
Contents	iii
List of Tables	vi
List of Figures	vii
Notations	1
Introduction	2
1 Basic principle of fluid mechanics	5
1.1 Description of motion	5
1.1.1 Description of Lagrange	5
1.1.2 Description of Euler	6
1.2 particle path	8
1.2.1 Streamlines	8
1.3 Fundamental Equations of motion of a fluid	8
1.3.1 Conservation of mass	9
1.3.2 Navier–Stokes equation	10
1.3.3 Euler equation	11
1.3.4 Bernoulli equation	11
1.4 Surface tension	12

1.5	Two-Dimensional Flows	14
1.6	Complex variable	17
1.6.1	Complex potential	17
1.6.2	Conformal mapping	17
1.6.3	Schwarz–Christoffel Theorem	18
1.6.4	Hodograph method	21
1.7	The basics of dimensional analysis	23
1.7.1	The Buckingham π theorem	24
1.7.2	Dimensionless numbers	24
2	Exact Solution of a two-dimensional jet flow past an infinite wedge problem	26
2.1	Mathematical formulation	27
2.1.1	Dimensionless variables	30
2.2	Exact solution of the problem	31
2.2.1	Free streamline forms for various values of β	39
3	Surface tension effects on jet flow past an infinite wedge	48
3.1	Formulation of the problem	51
3.2	Conformal mapping	51
3.3	Boundary integral approach	57
3.3.1	Numerical procedure	58
3.3.2	Cartesian coordinates of the free surface	59
3.3.3	Free surface profiles	60
4	Nonlinear Free Surface Flow past a Wedge in Channel	66
4.1	Introduction	66
4.2	Formulation of the problem	69
4.3	Numerical procedure	72
4.4	Discussion of results	75

<i>CONTENTS</i>	v
4.4.1 Flow with surface tension effect	76
4.4.2 Solution for large $T(\alpha \rightarrow 0)$	77
4.4.3 Flow without surface tension.	77
general conclusion	86
Bibliography	87

List of Tables

4.1	The positioning of the major points of the flow domain problem in the f-plane and the t-plane	74
4.2	Some values of the coefficients a_n of the series (4.21) for several values of the angle β , $b = b' = 0.5$ and different values of Weber number α	76
4.3	Some values of the minimal Weber number for and different values of the wedge angle	76

List of Figures

1.1	The effect surface tension force	13
1.2	The velocity vector \vec{V} is tangential to the streamline	15
1.3	w-plane	19
1.4	z-plane	20
2.1	Jet past an infinite wedge in z-plane	28
2.2	Flow past a semi infinite plate in z-plane	29
2.3	Flow domain in the Hodograph plane	32
2.4	The free surface shape for $\frac{\pi}{3}$	44
2.5	The free surface shape for $\frac{\pi}{2}$	45
2.6	The free surface shape for $\frac{2\pi}{3}$	46
3.1	z-plane	50
3.2	f-plane	54
3.3	ζ -plane	55
3.4	ζ -plane	56
3.5	Comparison of the analytical solution and the numerical solution for $\frac{\pi}{6}$	61
3.6	Comparison of the analytical solution and the numerical solution for $\frac{\pi}{2}$	62
3.7	Free streamline shapes for $\frac{2\pi}{3}$ and various Weber numbers α	63
3.8	Free streamline shapes for $\frac{\pi}{2}$ and various Weber numbers α	64
3.9	Free streamline shapes for $\frac{\pi}{3}$ and various Weber numbers α	65

4.1	Sketch of the flow past a wedge and of the coordinates The wedge angle is β , the width of the channel is $2H_0$ and the depth of the flow at infinity is $H + H'$. The x-axis is along the streamline EOF and the y vertically through the point.	68
4.2	Flow configuration in the complex potential f-plane.	70
4.3	The image of the Flow in the t-plane.	73
4.4	Coefficients of contraction C and C' vs $\frac{1}{\alpha}$	79
4.5	The angles of separation γ and γ' vs $\frac{1}{\alpha}$	80
4.6	Computed free streamline shapes for $\beta = \frac{3\pi}{2}$, $b = b' = 0,5$ and various Weber numbers	81
4.7	Computed free streamline shapes for $\beta = \pi$, $b = b' = 0,5$ and various Weber numbers.	82
4.8	Compued free streamline shapes for $\beta = \frac{\pi}{2}$, $b = b' = 0,5$ and various Weber numbers	83
4.9	Comparison of the obtained results of $C = C'$ for various values of β and $b = b' = 0,5$ with the experimental and theoretical results given in [7]. . . .	84
4.10	Comparison of the calculated free surface with the exact solution for $\beta = \pi$, $b = b' = 1$	85

Notations

ψ	two-dimensional flow stream function
ϕ	velocity potential
μ	dynamic viscosity
Fr	Froude number
α, We	Weber number
ρ	density
T	surface tension
H	depth, amplitude
\vec{F}_V	volume force
g	gravity acceleration constant
p	fluid pressure
ζ	complex velocity
f	complex potential
x	Cartesian coordinate
y	Cartesian coordinate
z	complex number
q	magnitude of the velocity
θ	argument of the complex velocity
u, v	Cartesian velocity components
$\vec{\nabla}, \overrightarrow{\text{grad}}$	gradient
Δ	Laplacian
div	divergence
$\overrightarrow{\text{curl}}$	rotation vector
$\frac{D}{Dt}, \frac{d}{dt}$	Absolute differential
$\frac{\partial}{\partial t}$	partial differentials
η	normal vector
α, β	apex angle
\vec{a}	acceleration

Introduction

The engineering discipline of fluid dynamics examines the pressures and energies produced by moving fluids. In order to comprehend the dynamics of fluid flow motion, hydrodynamics entails applying the basic concepts of mechanics and thermodynamics. In daily life, fluid dynamics and hydrodynamics are crucial. Examples from daily life include the airflow in the kitchen sink, the exhaust fan over the range, and our home's air conditioning unit. When we drive a car, air flow around the car's body creates some drag, which grows with the square of the vehicle's speed and adds to fuel usage. Applications for engineering include the movement of fluid in pipelines and canals, the production of energy, environmental processes, and transportation (cars, ships, aircrafts). Coastal uses are among the others uses include fluid motion in the human body, wind flow around buildings, fluid circulation in lakes, oceans, and the atmosphere. The movement of fluids is modeled with complex mathematical equations, including the Navier-Stokes equation. which is difficult to find its general solution, and the state of existence and uniqueness of the solution in the general case. As for special cases, we find exact solutions for them in simple and few cases, and most other cases are solved numerically using several methods, including: Series truncation method, Boundary integral method, finite volume, finite element , finite difference,.... Our research focuses on the analytical and numerical analysis of two-dimensional flow in the intersection of straight walls , flow over obstacles and jets impinging on the walls. This work builds upon previous research conducted by M.I. Gurevich[20], Birkhoff, G., E.H. Zarantonello[6], and L.M. Milne-Thomson[26], who found exact solutions in the case of neglecting gravity and surface tension force. One of the issues they addressed is

the flow of a liquid from a jet orifice and under gravity from a sluice gate. Their solution method is based on finding a one-to-one mapping function that coherently maps the flow on the inner half of a disk. Since the complex potential is known by the corresponding flux in one half of the disk, the form of the mapping function can be obtained by considering the velocity terms. By using the form of the assignment function and the fact that pressure is constant over free flow, the problem of determining the required transformation can be reduced to solving a nonlinear integral equation. L.M. Milne-Thomson proposed this method of reducing the problem to an integral equation. After the advent of computers, these problems became solved numerically, and J.-M. Vanden-Broeck[38] solved a large number of them and used the sequential truncation method. He used it in fountains and fluid flow around obstacles, and examine two-dimensional flows in a domain with a vertical wall, a free surface, a semi-infinite horizontal wall, and an infinite horizontal wall above. Gravity is considered, and the fluid is believed to be incompressible and inviscid. Series truncation is used to numerically fix the problem., followed by A. C. King and M. I. G. Bloor[[22],[23]], where he found the numerical solution for the free surface flow through a step and an arbitrary bed topography. There is a lot of research in the field of fluid mechanics, with many researchers exploring different aspects of fluid dynamics problems. It seems that many of these researchers have used a variety of mathematical techniques to address these issues, including integro-differential equations, Fourier's double-integral theorem, the Hilbert Method, and perturbation techniques. It's also interesting to note that some researchers have focused on specific types of obstacles or configurations, such as semi-circular or triangular obstacles, ramps, trapezoidal bottoms, sluice gates, and jets passing through wedges. of these researchers Abd-el-Malek, Mina B and Hanna, Sarwat N[1], Smith, AC and Lim, TH[32], Semenov, YA and Wu, GX[30] etc... In this work, I addressed the nonlinear case characterized by Bernoulli's equation on the free surface, which is in the form of an unknown surface. By neglecting the effect of surface tension, we applied the Hodograph method to solve this problem analytically. However, when taking surface tension into account, the problem becomes very difficult to solve analytically, making it essential to find an approximate solution. In this thesis, I discussed the problem of a two-dimensional

jet passing through a infinite wedge, utilizing the Hodograph method. This method was applied by Rutherford in the vertical case of a flat plate, and a lot of research on this problem has been conducted, including works by M.J. Cooker [11], Weidong Peng and David F Parker[28], B Bouderah, A Gasmi, and H Serguine[8], Merzougui A, and Mekias H and Guechi, F [25]. The other topic addressed in this work is a two-dimensional problem of an asymmetric wedge located in a channel, characterized by nonlinearity. This problem has been extensively studied under the assumption of neglecting the forces of gravity and surface tension by many researchers, including T Yao-Tsu Wu, Arthur K Whitney, and Christopher Brennen[40], Gurevich, M. I[20], R. J Hureau and R Weber[21], Birkhoff, G., and E.H. Zarantonello[6]. The boundary conditions on the free surface of the unknown equation were solved numerically using series truncation technique. Our work consists of four chapters:

Chapter 1: Preliminary concepts related to fluid flows, including two-dimensional potentials, current lines (streamlines and potential lines), and basic fluid motion equations.

Chapter 2: Examination of the two-dimensional potential flow problem of an incompressible liquid produced by a jet effect on an infinitely wedge-shaped wall, neglecting the effects of surface tension and gravity. In this case, we seek the analytical expression for the free surface equation. The problem is solved analytically using the hodograph method for some familiar angles.

Chapter 3: Consideration of the same problem with the effect of the force of surface tension. In this case, the problem is characterized by a Weber number, and we adopt the numerical method of the differential integral equation. The problem is reduced to an algebraic system of nonlinear equations that are solved by Newton's method.

Chapter 4: Investigation of the problem of the effect of a wedge placed in an infinite straight tunnel on the fluid flow inside the channel, taking into account the effect of surface tension. In this case, we solve this problem numerically by using series truncation.

Chapter 1

Basic principle of fluid mechanics

When describing the state of a moving fluid, you can determine a number of physical properties at each point, including pressure, density, and speed. All of these properties depend on the coordinates x, y , and z , and they change over time.

1.1 Description of motion

The fluid particle is chosen as an elementary entity allowing a complete description of the flows; it is a "package" of molecules surrounding a given point that moves with the fluid. The fluid particle is characterized from the thermodynamic point of view by its density ρ , its pressure p and its temperature T . For the study of the movement, one introduces the position and the speed of the particle which translates, turns on itself and deforms when it flows.

1.1.1 Description of Lagrange

This method of describing the flow involves tracking a specific particle as it moves through the stream. The ability to describe mobility is made possible by how the particle positions have changed over time. At each instant, there corresponds a position of P . The coordinates $x = x(t), y = y(t), z = z(t)$ of the particle P are called Lagrange variables. The

instantaneous velocity vector of the particle P is:

$$\begin{aligned}\vec{v} &= \frac{d \vec{op}}{dt} = \frac{dx}{dt} \vec{i} + \frac{dy}{dt} \vec{j} + \frac{dz}{dt} \vec{k} \\ &= v_x \vec{i} + v_y \vec{j} + v_z \vec{k}\end{aligned}\quad (1.1)$$

Where the \vec{i}, \vec{j} , and \vec{k} are the unit vectors of the axes of the reference system. The trajectories are defined by the coordinates x, y, z of the particle as a function of time and of the initial conditions at time t_0 , i.e

$$\begin{aligned}x &= f_1(x_0, y_0, z_0, t) \\ y &= f_2(x_0, y_0, z_0, t) \\ z &= f_3(x_0, y_0, z_0, t)\end{aligned}\quad (1.2)$$

The instantaneous acceleration is the ratio of the speed variation over the duration studied when this duration tends towards 0. In other words, the acceleration is the derivative of the speed and therefore the second derivative of the position.

$$\begin{aligned}\vec{a} &= \frac{d \vec{v}}{dt} \\ &= \frac{dv_x}{dt} \vec{i} + \frac{dv_y}{dt} \vec{j} + \frac{dv_z}{dt} \vec{k} \\ &= \frac{d^2 x}{dt^2} \vec{i} + \frac{d^2 y}{dt^2} \vec{j} + \frac{d^2 z}{dt^2} \vec{k} \\ &= a_x \vec{i} + a_y \vec{j} + a_z \vec{k}\end{aligned}\quad (1.3)$$

1.1.2 Description of Euler

This description of the flow consists in establishing at a given time t the set of velocities associated with each point in the space occupied by the fluid. At each instant t , the fluid flow is described by means of a velocity vector field.

The components v_x, v_y, v_z of the velocity \vec{v} in the chosen reference frame are functions of four independent variables (x, y, z) and t , called Euler variables.

This method of description is preferably used. At each point $M(x, y, z)$ in space, identified with respect to a fixed system, we observe the passage of particles over time. We are not interested in the changing identities of the particles, but in the speed $\vec{v}(t)$ possessed by the particle which pass at time t . The value of any function of the flow field expressed in Euler variables $f(x, y, z, t)$ therefore corresponds to the fluid particle located at the point (x, y, z) at time t considered.

To know the acceleration, it is necessary to follow the fluid particle for an infinitesimal duration.

The speed being a function with multiple variables, themselves all function of time, this expression is that of a particulate derivative (particular case of total derivative). It makes it possible to take into account not only the local variation of the speed over time but also the variation of the latter linked to the displacement of the particle.

$$\vec{a}(\vec{r}, t) = \frac{d \vec{v}(\vec{r}, t)}{dt} \quad (1.4)$$

$$\vec{r} = \begin{pmatrix} x(t) \\ y(t) \\ z(t) \end{pmatrix}, \text{The position of the fluid particle at the moment } t.$$

The acceleration can then be expressed, by making the variables implicit:

$$\begin{aligned} \vec{a} &= \frac{d \vec{v}}{dt} \\ &= \frac{\partial \vec{v}}{\partial t} + \frac{\partial \vec{v}}{\partial x} \frac{dx}{dt} + \frac{\partial \vec{v}}{\partial y} \frac{dy}{dt} + \frac{\partial \vec{v}}{\partial z} \frac{dz}{dt} \\ &= \frac{\partial \vec{v}}{\partial t} + v_x \frac{dx}{dt} + v_y \frac{dy}{dt} + v_z \frac{dz}{dt} \\ &= \frac{\partial \vec{v}}{\partial t} + (\vec{v} \cdot \vec{\nabla}) \cdot \vec{v} \\ &= \frac{\partial \vec{v}}{\partial t} + \frac{1}{2} \vec{\nabla} v^2 + (\vec{\nabla} \wedge \vec{v}) \wedge \vec{v} \end{aligned} \quad (1.5)$$

1.2 particle path

It is the collection of points that a fluid particle has inhabited over time. In math, we can write: $\overrightarrow{OM} = \vec{r} = f(\vec{r}_0, t)$, where \vec{r}_0 is the particle's starting position at time $t = 0$. Therefore, this is referred to as Lagrangian tracking (following the displacement of a given object over time). By definition, the trajectory's tangent is parallel to the particle's velocity vector as it passed through this location. An age-old method for obtaining the trajectory is to take a picture with a long exposure while constantly lighting the flow.

1.2.1 Streamlines

The streamline is the curve which, at each of its points, is always tangential to the velocity vector of the flow field. It is expressed by the differential equation:

$$\frac{dx}{dv_x(x, y, z, t)} = \frac{dy}{dv_y(x, y, z, t)} = \frac{dz}{dv_z(x, y, z, t)} \quad (1.6)$$

For an infinitely small displacement \overrightarrow{dM} of the point M on a streamline, we can write:

$$\vec{v} \wedge \overrightarrow{dM} = \vec{0}$$

Which is written scalarally:

$$\begin{cases} v_y dx - v_x dy = 0 \\ v_y dz - v_z dy = 0 \\ v_z dx - v_x dz = 0 \end{cases} \quad (1.7)$$

1.3 Fundamental Equations of motion of a fluid

The following laws of conservation are included in the collection of dynamic equations that describe the motion of continuum:

1. The equation of conservation of mass of continuum.
2. The law of conservation of momentum.
3. The equations of angular momentum.
4. The law of conservation of energy.

1.3.1 Conservation of mass

The mass in a control volume is written:

$$M_{VC} = \int \int \int_{VC} \rho(\vec{r}, t) d\tau \quad (1.8)$$

Here, ρ is the density.

If there is conservation of mass then:

$$\frac{dM_{VC}}{dt} = 0 \quad (1.9)$$

By applying the Green-Ostrogradsky theorem

$$\begin{aligned} \frac{d}{dt} \int \int \int_{VC} \rho(\vec{r}, t) d\tau &= \int \int_{SC} \frac{\partial \rho}{\partial t} + \int \int_{SC} \rho(\vec{r}, t) \vec{v} \cdot \vec{ds} \\ &= \int \int \int_{VC} \left[\frac{\partial \rho}{\partial t} + \text{div}(\rho \vec{v}) \right] d\tau \end{aligned} \quad (1.10)$$

This equation is true for any volume VC , and consequently the integrand is zero, hence:

$$\frac{\partial \rho}{\partial t} + \text{div}(\rho \vec{v}) = 0 \quad (1.11)$$

called (1.9) conservation de la masse sous forme locale.

By developing the divergence term

$$\text{div}(\rho \vec{v}) = \rho \text{div}(\vec{v}) + \vec{v} \cdot \vec{\nabla} \rho \quad (1.12)$$

Special case of an incompressible fluid

For an incompressible flow (i.e. $\rho = \text{constant}$) the continuity equation becomes:

$$\text{div}(\vec{v}) = 0 \quad (1.13)$$

1.3.2 Navier–Stokes equation

For a Newtonian incompressible fluid, the dynamics of the flow verifies the equation

Conservation of momentum

$$\rho \left(\frac{\partial \vec{v}}{\partial t} + (\vec{v} \cdot \vec{\nabla}) \vec{v} \right) = -\vec{\nabla} p + \rho \vec{F}_V + \mu \Delta \vec{v} \quad (1.14)$$

μ is the dynamic viscosity coefficient of the fluid

\vec{F}_V is volumetric forces for the gravity force

$\vec{F}_V = -\overrightarrow{\text{grad}}(U)$ where $U = gz$.

p is pressure

For a two-dimensional flow and gravity forces, the Navier-Stokes equation is:

$$\rho \left(\frac{\partial v_x}{\partial t} + v_x \frac{\partial v_x}{\partial x} + v_y \frac{\partial v_x}{\partial y} \right) = -\frac{\partial}{\partial x} (p + \rho gz) + \mu \left(\frac{\partial^2 v_x}{\partial x^2} + \frac{\partial^2 v_x}{\partial y^2} \right) \quad (1.15)$$

$$\rho \left(\frac{\partial v_y}{\partial t} + v_x \frac{\partial v_y}{\partial x} + v_y \frac{\partial v_y}{\partial y} \right) = -\frac{\partial}{\partial y} (p + \rho gz) + \mu \left(\frac{\partial^2 v_y}{\partial x^2} + \frac{\partial^2 v_y}{\partial y^2} \right) \quad (1.16)$$

For an ideal fluid flow the Navier-Stokes equation(1.14) becomes:

$$\rho \left(\frac{\partial \vec{v}}{\partial t} + (\vec{v} \cdot \vec{\nabla}) \vec{v} \right) = -\vec{\nabla} p + \rho \vec{F}_V \quad (1.17)$$

Finally : The local equations of motion of a perfect incompressible fluid are written:

$$\begin{cases} \text{div}(\vec{v}) = 0 \\ \rho \left(\frac{\partial \vec{v}}{\partial t} + (\vec{v} \cdot \vec{\nabla}) \vec{v} \right) = -\vec{\nabla} p + \rho \vec{F}_V \end{cases} \quad (1.18)$$

For a two-dimensional flow and gravity forces, the Navier-Stokes equation(1.17) written in cartesian coordinates is:

$$\rho \left(\frac{\partial v_x}{\partial t} + v_x \frac{\partial v_x}{\partial x} + v_y \frac{\partial v_x}{\partial y} \right) = -\frac{\partial}{\partial x} (p + \rho gz) \quad (1.19)$$

$$\rho \left(\frac{\partial v_y}{\partial t} + v_x \frac{\partial v_y}{\partial x} + v_y \frac{\partial v_y}{\partial y} \right) = -\frac{\partial}{\partial y} (p + \rho gz) \quad (1.20)$$

Where z is the height and is a positive, vertically upward.

1.3.3 Euler equation

We neglect viscosity, then ($\mu = 0$) and we obtain the Euler equation

$$\rho \left(\frac{\partial \vec{v}}{\partial t} + (\vec{v} \cdot \vec{\nabla}) \vec{v} \right) = -\vec{\nabla} p + \rho \vec{F}_v \quad (1.21)$$

Euler's equation can be written in another form

$$\rho \left(\frac{\partial \vec{v}}{\partial t} + (\vec{v} \cdot \vec{\nabla}) \vec{v} \right) = -\vec{\nabla} (p + \rho g z) \quad (1.22)$$

We use the derivative property of the scalar product of vectors

$$\vec{\nabla}(\vec{A} \cdot \vec{B}) = \vec{A} \wedge \overrightarrow{curl}(\vec{B}) + \vec{B} \wedge \overrightarrow{curl}(\vec{A}) + (\vec{A} \cdot \vec{\nabla}) \vec{B} + (\vec{B} \cdot \vec{\nabla}) \vec{A} \quad (1.23)$$

If we write it for the vector $\vec{A} = \vec{B} = \vec{v}$ we obtain:

$$(\vec{v} \cdot \vec{\nabla}) \vec{v} = \vec{\nabla} \left(\frac{v^2}{2} \right) - \vec{v} \wedge \overrightarrow{curl}(\vec{v}) \quad (1.24)$$

Euler's equation(1.22) is then written:

$$\rho \frac{\partial \vec{v}}{\partial t} = -\vec{\nabla} \left(p + \frac{v^2}{2} + \rho g z \right) + \vec{v} \wedge \overrightarrow{curl}(\vec{v}) \quad (1.25)$$

1.3.4 Bernoulli equation

If the flow is irrotational and permanent (stationary) then $\overrightarrow{curl}(\vec{v}) = \vec{0}$; $\frac{\partial \vec{v}}{\partial t} = \vec{0}$ in equation(1.25) becomes:

$$\vec{\nabla} \left(p + \frac{v^2}{2} + \rho g z \right) = \vec{0} \quad (1.26)$$

The final integrated form of the equation (1.26) is the Bernoulli equation,for flow:

$$p + \frac{v^2}{2} + \rho g z = C \quad (1.27)$$

Bernoulli's equation then shows that the total pressure remains constant along the same streamline because \vec{v} is at any point tangent to a streamline.

1.4 Surface tension

They are surface forces that work to make the liquid droplets take the spherical shape, which means that the surface of the liquid has more energy than the rest of the liquid parts, which is used to reduce the surface area. For molecules inside the liquid, the net force is zero, while for molecules on the surface, the net force acting on them is not zero and is in a downward direction. So Surface tension is the perpendicular forces that affect the unit lengths of the surface of the liquid and pull it downward, and its unit is N/m - Newton per meter. Consider a small spot on the free surface of the liquid. The angle opposite arcs \widehat{AB} and \widehat{BC} at the center of curvature is $d\theta$. The sum of the forces at the two end points is all that is required to determine the surface tension force operating on this element in the normal direction.

$$\text{Net force} = 2T \sin d\theta \quad (1.28)$$

As $ds \rightarrow 0, d\theta \rightarrow 0$ and so there is a force

$$2T \sin \theta \approx 2Td\theta \quad (1.29)$$

targeted at BO . Due to the pressure difference across the free surface, a force must counteract this force. This is the case because a massless element is being affected by the pressures. Inputting force components along the normal OB and letting p be the fluid pressure and p_a be the air pressure results in

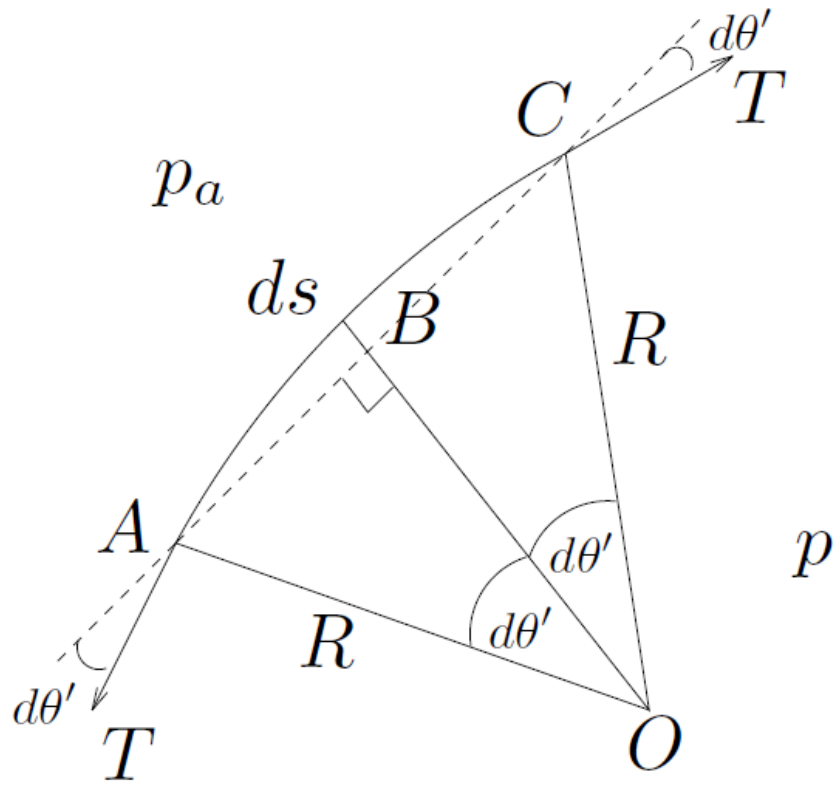


Figure 1.1: The effect surface tension force

$$2T d\theta = (p - p_a) ds \quad (1.30)$$

The surface element length can be written in terms of the radius R and the angle $d\theta$ by another result of taking into account $ds \rightarrow 0$

$$ds = 2R d\theta \quad (1.31)$$

The result of changing (1.31) to (1.30) is

$$(p - p_a) ds = \frac{T}{R} ds \implies (p - p_a) = \frac{T}{R} = TK \quad (1.32)$$

where $K = \frac{1}{R}$ is the curvature, which is positive if the free surface at B is convex when viewed from the air side of B , as shown in figure(1.1). If B is curved, $K = \frac{1}{R}$ is negative. When (1.32) is substituted for (1.27), the result is used on the free surface.

$$\frac{v^2}{2} + \frac{TK}{\rho} + \rho g z = C$$

where the Bernoulli constant has absorbed the steady atmospheric pressure.

1.5 Two-Dimensional Flows

For two-dimensional, irrotational flows of an ideal fluid, the main results can be summarized as follows: The condition for the flow to be incompressible is given by:

$$\text{div}(\vec{V}) = 0 \quad (1.33)$$

where $\vec{V} = (u, v)$, and this condition can be expressed as:

$$\frac{\partial u}{\partial x} + \frac{\partial v}{\partial y} = 0 \quad (1.34)$$

The flow is irrotational, which implies:

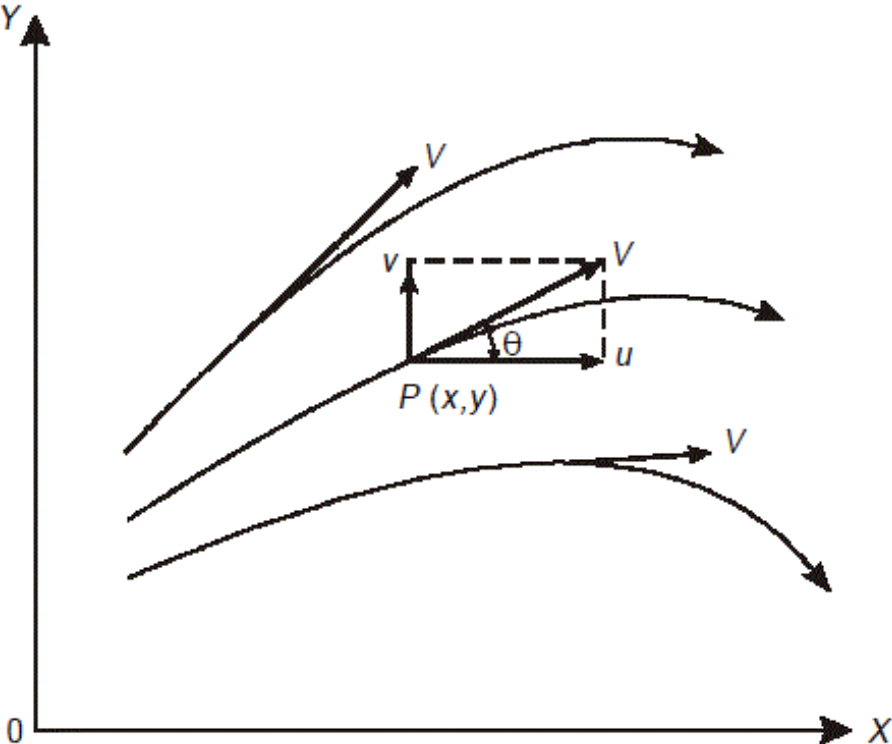


Figure 1.2: The velocity vector \vec{V} is tangential to the streamline

$$\overrightarrow{curl}(\overrightarrow{V}) = \overrightarrow{0} \quad (1.35)$$

This condition can be expressed as:

$$\frac{\partial v}{\partial x} - \frac{\partial u}{\partial y} = 0 \quad (1.36)$$

According to equation(1.7)becomes

$$udy - vdx = 0 \quad (1.37)$$

So, according to the total derivation theory, At least there is a function ψ where

$$d\psi = udy - vdx \quad (1.38)$$

the ψ is one which satisfies

$$\begin{cases} u = \frac{\partial \psi}{\partial y} \\ v = -\frac{\partial \psi}{\partial x} \end{cases} \quad (1.39)$$

From equation(1.37) we find

$$d\psi = 0 \quad (1.40)$$

Thus, along each streamline the function ψ has a constant value the streamline passing through the point $p(x, y)$ is tangential to the velocity vector \overrightarrow{V} at p According to equation (1.37) and figure(1.2) becomes

$$\frac{v}{u} = \frac{dy}{dx} = \tan(\theta) \quad (1.41)$$

By letting, this equation can be fulfilled.

$$\overrightarrow{V} = u \overrightarrow{i} + v \overrightarrow{j} \quad (1.42)$$

$$= \overrightarrow{\nabla} \phi \quad (1.43)$$

$$= \frac{\partial \phi}{\partial x} \overrightarrow{i} + \frac{\partial \phi}{\partial y} \overrightarrow{j}$$

where ψ, ϕ are called the stream function and potential function respectively . the two functions ψ, ϕ can be related by combining the results from (1.39) and (1.42) to give

$$\frac{\partial \phi}{\partial x} = \frac{\partial \psi}{\partial y} \text{ and } \frac{\partial \phi}{\partial y} = -\frac{\partial \psi}{\partial x} \quad (1.44)$$

The Cauchy-Riemann equations from the theory of functions of complex variables are the same shape as the two relations in(1.44). It is simple to demonstrate that the Laplace equation is satisfied by both the stream function $\psi(x, y)$ and the velocity potential $\phi(x, y)$. Combining formula (1.44) and the irrotational flow condition (1.34) results in

$$\frac{\partial^2 \psi}{\partial x^2} + \frac{\partial^2 \psi}{\partial y^2} = 0 \quad (1.45)$$

Similarly, applying (1.44) and the continuity requirement, we obtain

$$\frac{\partial^2 \phi}{\partial x^2} + \frac{\partial^2 \phi}{\partial y^2} = 0 \quad (1.46)$$

1.6 Complex variable

1.6.1 Complex potential

From equations (1.44) we known the complex potential f by

$$f(z) = \phi(z) + i\psi(z), \text{ wher } z = x + iy \quad (1.47)$$

From the Cauchy Riemann condition (1.44) We conclude that, f is an analytic function of $z - plane$. The complex velocity is defined as:

$$w = \frac{df}{dz} = u - iv = qe^{-i\theta} \quad (1.48)$$

where $q = \sqrt{u^2 + v^2}$ is the magnitude of the velocity. and θ is The argument of the complex velocity.

$$\theta = \arg(w) = \arctan\left(\frac{v}{u}\right) \quad (1.49)$$

1.6.2 Conformal mapping

The flow net on a w -diagram is always made up of a grid that is aligned to the - and -lines. Equipotentials are represented by vertical lines, while flows are represented by horizontal lines. As a consequence, the w -representation diagram's of flow is that of an infinite

fluid flowing uniformly in one direction: horizontal . Since the flow net in the w -plane is constant, the specific configuration in the z -plane solely relies on the transformation $w = f(z)$. The indirect approach of examining various functions to identify the type of boundaries to which they might apply is used to solve two-dimensional flow issues. The conformal transformation is the equation $w = f(z)$. Conformal mapping describes the transformation of the z -diagram to the w -diagram. The inverse transformation is defined as the function that transforms w into z , ($z = f^{-1}(w)$). The inverse transformation can be used to create numerous practical flow networks. It must be emphasized that the z -flow net and the w -flow net are completely unrelated. But occasionally it is impossible to solve the inverse function for W directly.

1.6.3 Schwarz–Christoffel Theorem

An significant mathematical finding is the Schwarz-Christoffel theorem, which enables a polygonal boundary in the w -plane to be mapped conformally onto the real axis, $y = 0$, in the z -plane. The area inside the polygon in the w -plane is typically mapped onto the upper half, $y > 0$, of the z -plane. The correct map is if the polygon's inner angles are $\alpha_1, \alpha_2, \dots$ and α_n .

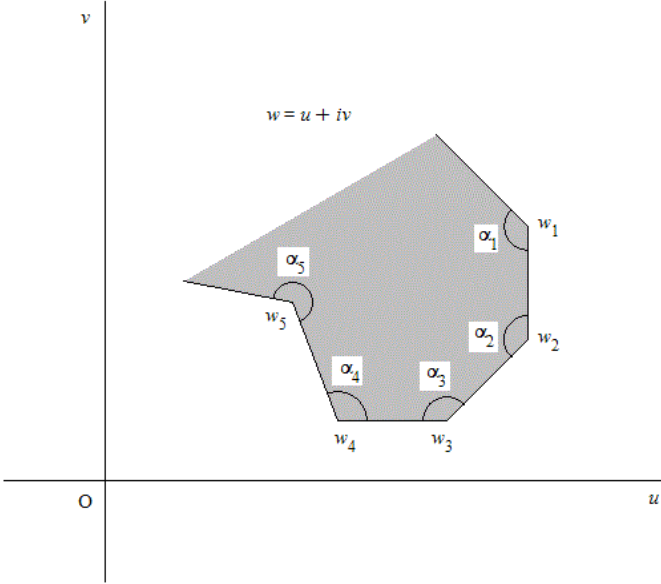


Figure 1.3: w-plane

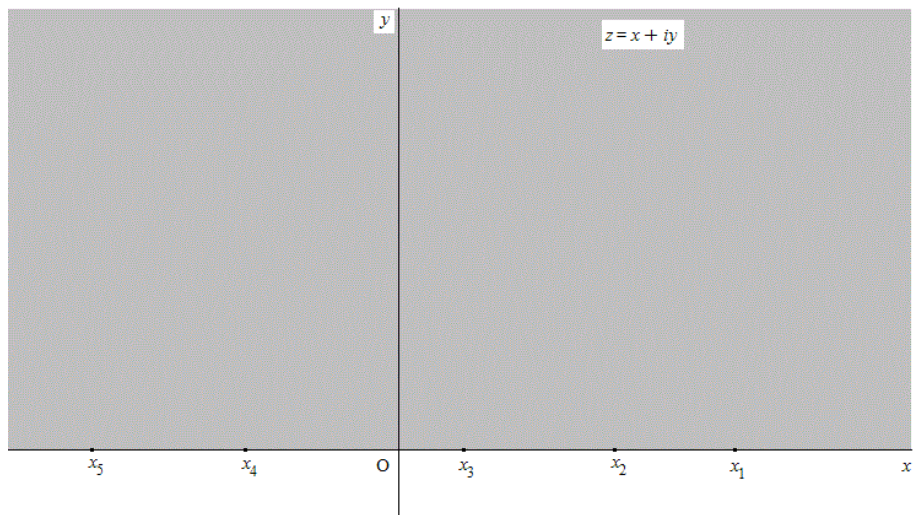


Figure 1.4: z-plane

The transformation is given by

$$\frac{dw}{dz} = A(z - x_1)^{\frac{\alpha_1}{\pi} - 1} (z - x_2)^{\frac{\alpha_2}{\pi} - 1} \dots (z - x_n)^{\frac{\alpha_n}{\pi} - 1} \quad (1.50)$$

where A is a complex number, and x_1, x_2, \dots, x_n are the real constants in z -plane that correspond to the

vertices of the polygon ascending order of magnitude; $\alpha_1, \alpha_2, \dots, \alpha_n$ are the interior angles of the polygon

We can integrate the previous expression(1.50) to give

$$w = A \int (z - x_1)^{\frac{\alpha_1}{\pi} - 1} (z - x_2)^{\frac{\alpha_2}{\pi} - 1} \dots (z - x_n)^{\frac{\alpha_n}{\pi} - 1} + B \quad (1.51)$$

where complex numbers A and B are used. While the complex number B decides where the polygon is in relation to the origin, the complex number A affects the polygon's size and orientation in the z -plane.

1.6.4 Hodograph method

The fundamental equations for the velocity components of a incompressible flow in terms of the space coordinates are nonlinear because the coefficients of the derivatives of the velocity components are themselves functions of the velocity.

Since there is no general method for solving the nonlinear differential equations, it is necessary, in the theoretical investigation of compressible flow problems to linearize the fundamental equations. For two-dimensional steady irrotational flow, the fundamental equations can be linearized by inverting the

roles of the dependent and the independent variables, i.e., by expressing the space coordinates or their equivalent in terms of the velocity components. Since the streamline in the plane with velocity components u and v as coordinates, i.e., hodograph plane, is known as hodograph, the method with u and v or q and θ as independent variables is called the hodograph method.

The quantity q is the magnitude of the velocity vector, and θ is the angle between

the velocity vector and the x -axis, i.e.,

$$u = q \cos \theta \text{ and } v = q \sin \theta \quad (1.52)$$

Initiating this method we go through the following steps

$$\begin{cases} f(z) = \phi + i\psi \\ \frac{df}{dz} = qe^{-i\theta} \end{cases} \quad (1.53)$$

we obtain

$$dz = \frac{e^{i\theta}}{q} df = \frac{e^{i\theta}}{q} \left(\frac{df}{dq} dq + \frac{df}{d\theta} d\theta \right) \quad (1.54)$$

Since (1.54) suggests that dz is a perfect differential,

$$\frac{\partial}{\partial \theta} \left(\frac{e^{i\theta}}{q} \frac{df}{dq} \right) = \frac{\partial}{\partial q} \left(\frac{e^{i\theta}}{q} \frac{df}{d\theta} \right) \quad (1.55)$$

from which we obtain

$$i \frac{\partial f}{\partial q} = \frac{-1}{q} \frac{\partial f}{\partial \theta} \quad (1.56)$$

equating real and imaginaries parts of (1.56), we obtain

$$\frac{\partial \phi}{\partial q} = \frac{-1}{q} \frac{\partial \psi}{\partial \theta} \text{ and } \frac{\partial \psi}{\partial q} = \frac{1}{q} \frac{\partial \phi}{\partial \theta} \quad (1.57)$$

from which we derive

$$\frac{\partial^2 \psi}{\partial q^2} + \frac{1}{q} \frac{\partial \psi}{\partial q} + \frac{1}{q^2} \frac{\partial^2 \psi}{\partial \theta^2} = 0 \quad (1.58)$$

If it is possible to specify the boundary conditions in terms of q and θ , equation (1.58) enables one to solve for

Using (1.57), one then solves for $\frac{df}{dq}$, $\frac{df}{d\theta}$. Using (1.54), one then determines $z = z(q, \theta)$, and next $x = x(q, \theta)$ and $y = y(q, \theta)$

1.7 The basics of dimensional analysis

The analysis of the engineering issue begins with developing the mathematical model based on the governing equations, which include conservation laws and secondary relations, and then seeking to solve this model and obtain a full understanding of the studied engineering case.

We will take an example, which is the problem of obstruction resulting from the flow of a fluid through a sphere

It is known for this case that the force of obstruction is D on a stable ball in a monotonous stream that is affected by the speed of the current U , the viscosity of the fluid μ , its density ρ , and the diameter of the ball d , from which we get

$$f(D, d, U, \rho, \mu) = 0 \quad (1.59)$$

To obtain the relationship between disability D and the other four variables in the laboratory, the direct method is to install three values of the four elements and conduct an experiment to determine the change of D with the fourth element, then repeat the experiment for the relationship of D with the other three elements separately. We note the difficulty of this direct method in experimental work because it

It takes a lot of effort and a long time if the number of items increases.

Difficulty or impossibility to install some elements and leave others to change.

For example: the change in viscosity is usually done by changing the fluid, but changing the fluid changes the density.

An alternative to this direct method of experimentation is to conduct experiments among dimensionless quantities made up of these elements rather than on the elements themselves.

We get the dimensionless quantity by multiplying or dividing the elements by each other so that the resulting quantity becomes dimensionless.

For example, the Reynolds number $Re = \frac{\rho U d}{\mu}$, and its components are given units $\frac{(kgm^{-3})(ms^{-1})(m)}{(kgm^{-1}s^{-1})}$, and thus its unit becomes 1, so it is therefore a dimensionless quantity.

How can we convert the governing elements of flow into non-dimensional quantities?
We follow what is known as the Buckingham theory.

1.7.1 The Buckingham π theorem

is a fundamental theorem in dimensional analysis

If a problem includes n number of physical variables:

$p_1, p_2, p_3, \dots, p_n$ where $f(p_1, p_2, p_3, \dots, p_n) = 0$,

and the elements include m dimensions combined, then the number of independent non-dimensional magnitudes is $n - m$.

which governs the phenomenon can be put in the form

$$f(\pi_1, \pi_2, \pi_3, \dots, \pi_{n-m}) = 0$$

where the $\pi_1, \pi_2, \pi_3, \dots, \pi_{n-m}$ are independent dimensionless variables

1.7.2 Dimensionless numbers

Froude number:

$$Fr = \frac{V}{\sqrt{gL}}$$

where g is the gravitational acceleration. The Froud number is important as the gravitational force has an estimated value compared to the other forces.

drag coefficient for a structural shape:

$$C_D = \frac{2\tau_0}{\rho V^2} = \frac{\text{shearstress}}{\text{dynamic pressure}}$$

where τ_0 is the shear stress (Pa);

Note: other notations include Cd and Cf ;

Reynolds number:

$$Re = \frac{\rho V \times d_{charac}}{\mu} = \frac{\text{inertial forces}}{\text{viscous forces}}$$

The Reynolds number stands out as an important quantity. Where the viscous effect is important compared to other effects

Weber number:

$$W_e = \frac{V^2}{\frac{\sigma}{\rho d_{charac}}} = \frac{\text{inertial forces}}{\text{surface tension forces}}$$

σ is the surface tension

Chapter 2

Exact Solution of a two-dimensional jet flow past an infinite wedge problem

A jet flow can be seen in many engineering problems and flow past an obstacle is one example of these problems. This kind of problems is difficult to resolve because of the shape of the free surface which is unknown. It is interesting to note that the problem of fluid flow past a wedge has been studied by many researchers using different approaches and methods. The exact solution of the problem of direct impact of two equal jets was calculated by D. E. Rutherford[29] and L.M. Milne-Thomson[26], while M.J. Cooker[11] studied the steady free surface of water turning in the interior of a wedge formed by two impermeable, plane walls. Weidong Peng and David F Parker [28] modeled the flow of a jet against an arbitrary curved impermeable wall and used the boundary integral method, while J Hureau and R Weber[21] used the Hilbert transform and the generalized Schwarz-Christoffel method to solve the flow angle problem. In this paper, the authors present a solution to the problem of flow past an infinite wedge by assuming that the influence of gravity relative to inertia is negligible. The fluid is assumed to be inviscid, incompressible, and the flow is irrotational. The mathematical solution can be obtained exactly via the hodograph transformation

method and numerically by using the series truncation method. Many authors have used this numerical method to study this problem, including J. Asavanat and Vanden-Broeck Jean-Marc[4], A. Gasmi and H. Mekias[14], A. Gasmi [[16] , [15]] and A. Merzougui, H. Mekias, and F. Guechi[25] etc..... The authors found that for each value of the apex angle of the wedge, there is a solution to this problem using the method considered, and they illustrate the representation of the surface profile.

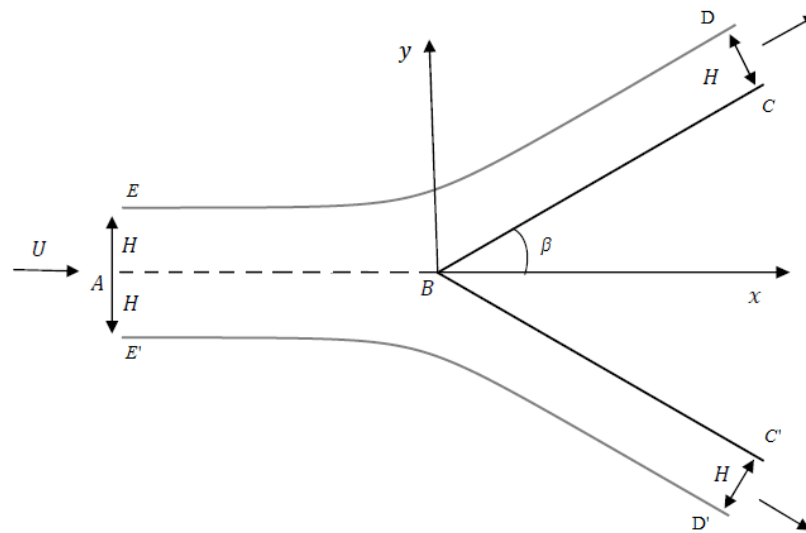
2.1 Mathematical formulation

The irrotational two-dimensional jet flow of an incompressible inviscid fluid past an infinite wedge is considered (see Figure 2.1). The effects of gravity is neglected. Far upstream the flow is uniform with a velocity U and amplitude H . The flow is limited by the walls of the wedge BC' and BC and the free surfaces. One chooses as coordinates the wall AB on x -axis and the y -axis is perpendicular and passing by B (see Figure 2.1). Because of the symmetry of the flow field, we need only consider the half of the flow region which is contained between the x -axis and the upper streamline(see Figure 2.2). The complex variable $z^* = x^* + iy^*$ is introduced.

A velocity potential denoted by ϕ^* and a stream function denoted by ψ^* are defined such that the complex potential is analytic in the domain occupied by the fluid. Bernoulli's equation is applied to both free surfaces on which pressure is constant, so that the fluid speed takes the constant value U there. Meanwhile the stream function ψ^* is chosen to have the value $-UH$ on the upper free surface and $\psi^* = 0$ along the streamline ABC . The relation between the complex potential and the complex velocity is given by

$$w^* = \frac{df^*}{dz^*} = u^* - iv^* = q^* e^{-i\theta} \quad (2.1)$$

$$f^* = \phi^* + i\psi^* \quad (2.2)$$

Figure 2.1: Jet past an infinite wedge in z -plane

Where is θ the angle between the flow direction and the x -axis and q^* is the magnitude of the velocity. So the the velocity components are given by:

$$\begin{cases} u^* = \frac{\partial\phi^*}{\partial x^*} = \frac{\partial\psi^*}{\partial y^*} \\ v^* = \frac{\partial\phi^*}{\partial y^*} = -\frac{\partial\psi^*}{\partial x^*} \end{cases} \quad (2.3)$$

2.1.1 Dimensionless variables

Before the problem can be solved, it is necessary to non-dimensionalise the variables so as to reduce the number of free parameters. This is done by using the upstream velocity U and the typical length H of Figure 2.1. The new, dimensionless variables are

$$z = x + iy = \frac{x^* + iy^*}{H}; \quad f = \phi + i\psi = \frac{\phi^* + i\psi^*}{UH}; \quad w = u - iv = \frac{u^* - iv^*}{U}; \quad q = \frac{q^*}{U} \quad (2.4)$$

So the potential function and stream function can be related by combining the results from (2.3) to give

$$\frac{\partial\phi}{\partial x} = \frac{\partial\psi}{\partial y} \quad \text{and} \quad \frac{\partial\phi}{\partial y} = -\frac{\partial\psi}{\partial x} \quad (2.5)$$

The two relations in (2.5) are in the same form as the Cauchy-Riemann equations from the theory of functions of complex variables.

This implies that the function f , where

$$f = \phi + i\psi \quad (2.6)$$

is an analytic function of $z = x + iy$. The function f is known as the complex potential.

it is possible to choose $\phi = 0$ at the wedge apex point origin B . and $\psi = 0$ along the streamline ABC . It then follows, from the choice of dimensionless variables, that $\psi = -1$ on the free surface ED By this the mathematical problem is to determine the variable ψ who verifies the following conditions:

$$\Delta\psi = 0 \quad (2.7)$$

$$\left(\frac{\partial\psi}{\partial x}\right)^2 + \left(\frac{\partial\psi}{\partial y}\right)^2 = 1, \quad (2.8)$$

on the free surface ED.

$$\frac{\partial\psi}{\partial y} = 0 \quad (2.9)$$

on the horizontal wall AB.

$$\frac{\partial\psi}{\partial y} = \frac{\partial\psi}{\partial x} \tan \beta \quad (2.10)$$

on the inclined wall BC.

2.2 Exact solution of the problem

In order to use the hodograph method we introduce the mapping

$$z \mapsto \zeta(z) = \frac{df}{dz} = u - iv = qe^{-i(\theta-\pi)} \quad (2.11)$$

where q and $(\theta - \pi)$ are the module and the argument of the velocity respectively. Under this mapping the image of the fluid domain in the hodograph plane is a sector of the disk such as the curve free streamline is mapped to a portion of the circle (see Figure 2.2).

We consider also the velocity potential ϕ and the stream function ψ as functions of (q, θ) We then have

$$dz = -\frac{e^{i\theta}}{q} df = -\frac{e^{i\theta}}{q} \left(\frac{\partial f}{\partial q} dq + \frac{\partial f}{\partial \theta} d\theta \right) \quad (2.12)$$

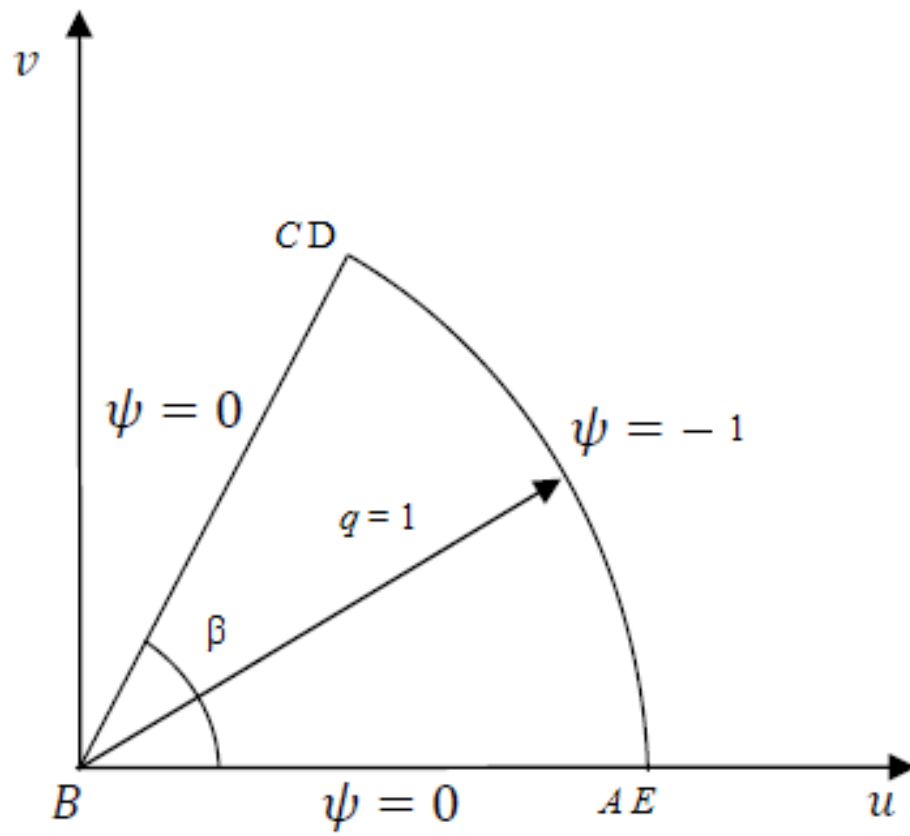


Figure 2.3: Flow domain in the Hodograph plane

since dz is a perfect differential, 2.12 implies:

$$\frac{\partial}{\partial \theta} \left(\frac{e^{i\theta}}{q} \frac{\partial f}{\partial q} \right) = \frac{\partial}{\partial q} \left(\frac{e^{i\theta}}{q} \frac{\partial f}{\partial \theta} \right) \quad (2.13)$$

from which we obtain

$$i \frac{\partial f}{\partial q} = \frac{-1}{q} \frac{\partial f}{\partial \theta} \quad (2.14)$$

equating real and imaginaries parts of (2.14), we obtain

$$\frac{\partial \phi}{\partial q} = \frac{-1}{q} \frac{\partial \psi}{\partial \theta} \quad \text{and} \quad \frac{\partial \psi}{\partial q} = \frac{1}{q} \frac{\partial \phi}{\partial \theta} \quad (2.15)$$

This equation is the fundamental equation of the hodograph method.

We may derive (2.15) for the velocity potential or the stream function. If we eliminate the velocity potential ϕ .

We find the equation for stream function of incompressible flow in the hodograph plane to be

$$\frac{\partial^2 \psi}{\partial q^2} + \frac{1}{q} \frac{\partial \psi}{\partial q} + \frac{1}{q^2} \frac{\partial^2 \psi}{\partial \theta^2} = 0 \quad (2.16)$$

we transform the boundary condition in the physical plane to a corresponding boundary condition in the hodograph plane.

In the hodograph plane the solution of the Eq.8 satisfies the streamlines $\psi = -1$, on sector of a circle DE and $\psi = 0$ on ABC . Noting that

$$\begin{cases} \psi(q, 0) = 0, & 0 < q \leq 1 \\ \psi(q, \beta) = 0, & 0 < q \leq 1 \end{cases} \quad (2.17)$$

$$\psi(1, \theta) = -1, \quad 0 < \theta < \beta \quad (2.18)$$

The separation variable technique is then used to resolve the aforementioned issue as described by Eq. (2.16) and the conditions (2.17) and (2.18).

Let

$$\psi(q, \theta) = R(q)\Theta(\theta) \quad (2.19)$$

solution to the problem

$$\begin{cases} \frac{\partial^2 \psi}{\partial q^2} + \frac{1}{q} \frac{\partial \psi}{\partial q} + \frac{1}{q^2} \frac{\partial^2 \psi}{\partial \theta^2} = 0, 0 < q < 1, 0 < \theta < \beta \\ \psi(q, 0) = \psi(q, \beta) = 0, 0 < q \leq 1 \\ \psi(1, \theta) = -1, 0 \leq \theta \leq \beta \end{cases} \quad (2.20)$$

where q alone determines R , and θ alone determines Θ . We first find R and Θ . to acquire, compute the ψ partial derivatives.

$$\frac{\partial \psi}{\partial q} = R'(q)\Theta(\theta); \quad \frac{\partial^2 \psi}{\partial q^2} = R''(q)\Theta(\theta); \quad \frac{\partial^2 \psi}{\partial \theta^2} = R(q)\Theta''(\theta) \quad (2.21)$$

These expressions (2.21) when entered into (2.16) yield

$$R''(q)\Theta(\theta) + \frac{R'(q)\Theta(\theta)}{q} + \frac{R(q)\Theta''(\theta)}{q^2} = 0 \quad (2.22)$$

and dividing factors produces

$$\frac{q^2 R''(q) + q R'(q)}{R(q)} = -\frac{\Theta''(\theta)}{\Theta(\theta)} \quad (2.23)$$

We can now see that the functions on the left side of (2.23) only rely on q , whereas the functions on the right side only depend on θ . The ratio on the right must remain constant C if we set q and vary θ .

$$\begin{cases} \frac{q^2 R''(q) + q R'(q)}{R(q)} = C \\ -\frac{\Theta''(\theta)}{\Theta(\theta)} = C \end{cases} \quad (2.24)$$

therefore

$$\begin{cases} q^2 R''(q) + q R'(q) - C R(q) = 0 \\ \Theta''(\theta) + C \Theta(\theta) = 0 \end{cases} \quad (2.25)$$

Equation (2.25) is called the Euler equation

In order to solve the two ordinary differential equations in (2.25) , we have reduced the issue of solving the partial differential equation to one with separable solutions (2.20). After that, we examine the border conditions in (2.17). Because these requirements are met by $\psi(q, \theta) = R(q)\Theta(\theta)$,

$$R(q)\Theta(0) = 0 \text{ and } R(q)\Theta(\beta) = 0; \quad 0 \leq q \leq 1 \quad (2.26)$$

Therefore, $R(q) = 0$ for $0 \leq q \leq 1$ or

$$\Theta(0) = 0 \text{ and } \Theta(\beta) = 0 \quad (2.27)$$

We create the boundary value problem by combining the boundary conditions in (2.27) with the differential equation for Θ in (2.25).

$$\begin{cases} \Theta''(\theta) + C\Theta(\theta) = 0 \\ \Theta(0) = \Theta(\beta) = 0 \end{cases} \quad (2.28)$$

We search for C numbers that lead to nontrivial solutions. We look at three three possible cases:

$$C = 0, \quad C < 0 \text{ and } C = \lambda^2 > 0 \quad (2.29)$$

Case1 $C = 0$, Here, the general solution is.

$$\Theta(\theta) = C_1 + C_2\theta \quad (2.30)$$

Using the boundary conditions(2.28), we get

$$C_1 = 0, \quad C_1 + C_2\beta = 0 \quad (2.31)$$

Therefore, $C_1 = C_2 = 0$, We get the trivial solution $\Theta(\theta) = 0$.

Case2 $C < 0$, Here, the general solution is.

$$\Theta(\theta) = C_1 e^{\sqrt{-C}\theta} + C_2 e^{-\sqrt{-C}\theta} \quad (2.32)$$

Given the boundary conditions(2.28) we have

$$\begin{cases} C_1 + C_2 = 0 \\ C_1 e^{\sqrt{-C}\beta} + C_2 e^{-\sqrt{-C}\beta} = 0 \end{cases} \quad (2.33)$$

We can see that the system's determinant (2.33), is not zero. Hence $C_1 = C_2 = 0$. We get the trivial solution $\Theta(\theta) = 0$

There is no interest because it is not important in our work.

Case3 $C = \lambda^2 > 0$, The general solution in this case is of the form.

$$\Theta(\theta) = C_1 \cos \lambda\theta + C_2 \sin \lambda\theta \quad (2.34)$$

The first boundary condition leads to

$$C_1 \cdot 1 + C_2 \cdot 0 = 0 \quad (2.35)$$

which implies

$$C_1 = 0 \quad (2.36)$$

Therefore, the second boundary condition becomes

$$C_2 \sin \lambda\beta = 0 \quad (2.37)$$

Clearly $C_2 \neq 0$, therefore

$$\sin \lambda\beta = 0 \quad (2.38)$$

which gives the eigenvalues

$$\lambda = \lambda_n = \frac{n\pi}{\beta}, \quad \text{for } n = 1, 2, 3, \dots \quad (2.39)$$

The value $n = 0$ is excluded because it leads to a trivial solution. Thus, the eigenfunctions

are given by

$$\Theta_n(\theta) = a_n \sin \frac{n\pi}{\beta} \theta, \text{ for } n = 1, 2, 3, \dots \quad (2.40)$$

where a_n are nonzero constants. The functions Θ_n are called eigenfunctions or modes

Now let us solve the R -equation. For $\lambda = \lambda_n = \frac{n\pi}{\beta}$ the equation is

$$q^2 R''(q) + qR'(q) - \left(\frac{n\pi}{\beta}\right)^2 R(q) = 0 \quad (2.41)$$

which is a Euler equation with general solution

$$R(q) = c_n q^{-\frac{n\pi}{\beta}} + d_n q^{\frac{n\pi}{\beta}} \quad (2.42)$$

Now since $\psi(q, \theta) < \infty$ as $q \rightarrow 0$ we require $c_n = 0$.

Thus, setting $d_n = 1$ for all n , we have

$$R(q) = q^{\frac{n\pi}{\beta}}, \text{ for } n = 1, 2, 3, \dots \quad (2.43)$$

In summary, we have constructed solutions of the given boundary value problem of the form

$$\psi_n(q, \theta) = a_n q^{\frac{n\pi}{\beta}} \sin \frac{n\pi}{\beta} \theta, \text{ for } n = 1, 2, 3, \dots \quad (2.44)$$

Now, to satisfy the boundary condition at $q = 1$ we form the linear combination

$$\psi(q, \theta) = \sum_{n=1}^{\infty} a_n q^{\frac{n\pi}{\beta}} \sin \left(\frac{n\pi\theta}{\beta} \right) \quad (2.45)$$

The boundary condition $\psi(1, \theta) = -1$ then yields

$$-1 = \sum_{n=1}^{\infty} a_n \sin\left(\frac{n\pi\theta}{\beta}\right) \quad (2.46)$$

Therefore, the coefficients are given by

$$a_n = -\frac{2}{\beta} \int_0^{\beta} \sin\left(\frac{n\pi\theta}{\beta}\right) d\theta \quad (2.47)$$

$$= \frac{2(\cos(n\pi) - 1)}{n\pi} \quad (2.48)$$

$$= \frac{2((-1)^n - 1)}{n\pi} \quad (2.49)$$

so that

$$a_n = \begin{cases} 0 & \text{if } n \text{ is even} \\ \frac{-4}{n\pi} & \text{if } n \text{ is odd} \end{cases} \quad (2.50)$$

By replacing the values of a_n in the equation (2.45), we obtain

$$\psi(q, \theta) = -\frac{4}{\pi} \sum_{n=0}^{\infty} \frac{1}{2n+1} q^{\frac{(2n+1)\pi}{\beta}} \sin\left(\frac{(2n+1)\pi\theta}{\beta}\right) \quad (2.51)$$

from the Cauchy-Riemann condition (2.5) and the relation of the stream function (2.51), we have thus, the complex potential is given by

$$\begin{aligned} \frac{\partial\phi}{\partial q} &= \frac{-1}{q} \frac{\partial}{\partial\theta} \left(-\frac{4}{\pi} \sum_{n=0}^{\infty} \frac{1}{2n+1} q^{\frac{(2n+1)\pi}{\beta}} \sin\left(\frac{(2n+1)\pi\theta}{\beta}\right) \right) \\ &= 4 \sum_{n=0}^{\infty} \frac{1}{\beta} q^{\frac{(2n+1)\pi}{\beta}-1} \cos\left(\frac{(2n+1)\pi\theta}{\beta}\right) \end{aligned} \quad (2.52)$$

By integration, we obtain the velocity potential :

$$\phi = \frac{4}{\pi} \sum_{n=0}^{\infty} \frac{1}{2n+1} q^{\frac{(2n+1)\pi}{\beta}} \cos\left(\frac{(2n+1)\pi\theta}{\beta}\right) \quad (2.53)$$

thus

$$f(q, \theta) = \phi(q, \theta) + i\psi(q, \theta) \quad (2.54)$$

Therefore, the potential function (2.53) take the form:

$$f(q, \theta) = \frac{4}{\pi} \sum_{n=0}^{\infty} \frac{1}{2n+1} q e^{-i\theta \frac{(2n+1)\pi}{\beta}} = \frac{4}{\pi} \sum_{n=0}^{\infty} \frac{1}{2n+1} \lambda^{\frac{(2n+1)\pi}{\beta}}, \quad \text{where } \lambda = q e^{-i\theta} \quad (2.55)$$

noting, from (2.12), that

$$dz = -\frac{df}{\lambda} = -\frac{4}{\beta} \sum_{n=0}^{\infty} \lambda^{\frac{(2n+1)\pi}{\beta}-2} d\lambda = -\frac{4}{\beta} \left(\frac{\lambda^{\frac{\pi}{\beta}-2}}{1 - \lambda^{\frac{2\pi}{\beta}}} \right) d\lambda \quad (2.56)$$

Now, from (2.56) Therefore integrating and observing that $z = 0$ when $\lambda = 0$ (the point stagnation), we get

$$z = -\frac{4}{\beta} \int_0^{\lambda} \frac{\lambda^{\frac{\pi}{\beta}-2}}{1 - \lambda^{\frac{2\pi}{\beta}}} d\lambda \quad (2.57)$$

On the bounding streamline $\psi = -1$, one has $q = 1$ or $\lambda = e^{-i\theta}$.

2.2.1 Free streamline forms for various values of β

Free Streamline for $\beta = \frac{\pi}{2}$

substitute this value in integral (2.57) we get:

$$\begin{aligned} z &= -\frac{8}{\pi} \int_0^{\lambda} \frac{1}{1 - \lambda^4} d\lambda \\ &= -\frac{2}{\pi} \left(\ln \left(\frac{1 + \lambda}{1 - \lambda} \right) + i \ln \left(\frac{1 - i\lambda}{1 + i\lambda} \right) \right) \end{aligned} \quad (2.58)$$

then

$$z = -\frac{2}{\pi} \left(\ln \left| \frac{1 + \lambda}{1 - \lambda} \right| + i \arg \left(\frac{1 + \lambda}{1 - \lambda} \right) + i \ln \left| \frac{1 - i\lambda}{1 + i\lambda} \right| + i \arg \left(\frac{1 - i\lambda}{1 + i\lambda} \right) \right) \quad (2.59)$$

On the free streamlines, $\lambda = e^{-i\theta}$; $0 < \theta < \frac{\pi}{2}$. thus

$$\begin{aligned}
\frac{1+\lambda}{1-\lambda} &= \frac{1+\cos\theta-i\sin\theta}{1-\cos\theta+i\sin\theta} \\
&= \frac{-i\sin\theta}{1-\cos\theta} \\
&= -\frac{1}{\tan\frac{\theta}{2}}i
\end{aligned} \tag{2.60}$$

and

$$\begin{aligned}
\frac{1-i\lambda}{1+i\lambda} &= \frac{1-\sin\theta-i\cos\theta}{1+\sin\theta+i\cos\theta} \\
&= \frac{-i\cos\theta}{1+\sin\theta} \\
&= -\frac{1-\tan\frac{\theta}{2}}{1+\tan\frac{\theta}{2}}i
\end{aligned} \tag{2.61}$$

We are finding the modulus and argument of two complex numbers $\frac{1+\lambda}{1-\lambda}$ and $\frac{1-i\lambda}{1+i\lambda}$.

$$\begin{aligned}
\left|\frac{1+\lambda}{1-\lambda}\right| &= \frac{1}{\tan\frac{\theta}{2}}; \text{ and } \arg\left(\frac{1+\lambda}{1-\lambda}\right) = -\frac{\pi}{2} \\
\left|\frac{1-i\lambda}{1+i\lambda}\right| &= \frac{1-\tan\frac{\theta}{2}}{1+\tan\frac{\theta}{2}}; \text{ and } \arg\left(\frac{1-i\lambda}{1+i\lambda}\right) = -\frac{\pi}{2}
\end{aligned} \tag{2.62}$$

And from it we get

$$\begin{aligned}
z &= -\frac{2}{\pi} \left(\ln\left(\frac{1}{\tan\frac{\theta}{2}}\right) - i\frac{\pi}{2} + i \ln\left(\frac{1-\tan\frac{\theta}{2}}{1+\tan\frac{\theta}{2}}\right) + \frac{\pi}{2} \right) \\
&= \frac{2}{\pi} \ln\left(\tan\frac{\theta}{2}\right) - 1 + i \left(-\frac{2}{\pi} \ln\left(\frac{1-\tan\frac{\theta}{2}}{1+\tan\frac{\theta}{2}}\right) + 1 \right)
\end{aligned} \tag{2.63}$$

where $t = \tan\frac{\theta}{2}$ and $0 < t < 1$

By separating the real parts and the imaginary parts, one obtains finally

$$\begin{cases} x = -1 + \frac{2\ln t}{\pi} \\ y = 1 - \frac{2\ln(\frac{1-t}{1+t})}{\pi} \end{cases} \tag{2.64}$$

This accords with ,Daniel Edwin Rutherford[29] and Milne-Thomson [26]

We will determine the free streamlines for the angles of $\frac{\pi}{3}$, $\frac{\pi}{4}$, $\frac{\pi}{6}$, $\frac{2\pi}{3}$, $\frac{3\pi}{4}$ and $\frac{5\pi}{6}$ using the same method.

Free Streamline for $\beta = \frac{\pi}{3}$

integral (19) becomes

$$z = \frac{1}{\pi} \left(\frac{-2\pi\sqrt{3}}{3} + 2 \ln(1 - \lambda^2) - \ln(\lambda^4 + \lambda^2 + 1) + 2\sqrt{3} \arctan \left(\frac{\sqrt{3}}{2\lambda^2 + 1} \right) \right) \quad (2.65)$$

On the free streamlines, $\lambda = e^{-i\theta}$, $0 < \theta < \frac{\pi}{3}$. thus

$$\begin{cases} x = \frac{-\sqrt{3}}{3} + \frac{4 \ln 2}{\pi} + \frac{1}{\pi} \ln \left(\frac{t^2}{(-3t^2+1)(-t^2+3)} \right) \\ y = 1 + \frac{\sqrt{3}}{\pi} \ln \left(\frac{(\sqrt{3}-t)(\sqrt{3}+3t)}{(\sqrt{3}+t)(\sqrt{3}-3t)} \right) \end{cases} \quad (2.66)$$

where $t = \tan \frac{\theta}{2}$ and $0 < t < \frac{\sqrt{3}}{3}$

Free Streamline for $\beta = \frac{\pi}{4}$

$$z = \frac{1}{\pi} \left(2 \ln \left(\frac{1-\lambda}{1+\lambda} \right) - \sqrt{2} \ln \left(\frac{\lambda^2 - \lambda\sqrt{2} + 1}{\lambda^2 + \lambda\sqrt{2} + 1} \right) + 4 \arctan(\lambda) + 2\sqrt{2} \arctan \left(\frac{\lambda\sqrt{2}}{\lambda^2 - 1} \right) \right)$$

On the free streamlines, $\lambda = e^{-i\theta}$; $0 < \theta < \frac{\pi}{4}$. thus

$$\begin{aligned} x &= 1 - \sqrt{2} - \frac{2\sqrt{2} \ln(1 + \sqrt{2})}{\pi} - \frac{1}{\pi} \left(\sqrt{2} \ln \left(\frac{(\sqrt{2}-1)^2 - t^2}{(\sqrt{2}+1)^2 - t^2} \right) - 2 \ln t \right) \\ y &= 1 - \frac{1}{\pi} \left(\sqrt{2} \ln \left(\frac{(\sqrt{2}-t)^2 - 1}{(\sqrt{2}+t)^2 - 1} \right) - 2 \ln \left(\frac{1-t}{1+t} \right) \right) \end{aligned}$$

where $t = \tan \frac{\theta}{2}$ and $0 < t < \sqrt{2} - 1$

Free Streamline for $\beta = \frac{\pi}{6}$

$$\begin{aligned} z &= \frac{1}{\pi} \left(2 \ln \left(\frac{1-\lambda}{1+\lambda} \right) + \ln \left(\frac{\lambda^2 - \lambda + 1}{\lambda^2 + \lambda + 1} \right) + \sqrt{3} \ln \left(\frac{\lambda^2 + \sqrt{3}\lambda + 1}{\lambda^2 - \sqrt{3}\lambda + 1} \right) - 4 \arctan \lambda - 2\sqrt{3} \arctan \left(\frac{\sqrt{3}\lambda}{\lambda^2 - 1} \right) \right. \\ &\quad \left. + 2 \arctan \left(\frac{\lambda}{\lambda^2 - 1} \right) \right) \end{aligned}$$

On the free streamlines, $\lambda = e^{-i\theta}$, $0 < \theta < \frac{\pi}{6}$. thus

$$\begin{aligned}
x &= \sqrt{3} - 2 + \frac{2\sqrt{3}\ln(2 - \sqrt{3})}{\pi} + \frac{1}{\pi} \left(\sqrt{3} \ln \left(\frac{(2 + \sqrt{3})^2 - t^2}{(-2 + \sqrt{3})^2 - t^2} \right) + \ln \left(\frac{1 - 3t^2}{3 - t^2} \right) + 2 \ln t \right) \\
y &= 1 + \frac{1}{\pi} \left(\sqrt{3} \ln \left(\frac{(\sqrt{3} - t)(\sqrt{3} - 3t)}{(\sqrt{3} + t)(\sqrt{3} + 3t)} \right) - \ln \left(\frac{3 - (t - 2)^2}{3 - (t + 2)^2} \right) - 2 \ln \left(\frac{1 - t}{1 + t} \right) \right)
\end{aligned}$$

where $t = \tan \frac{\theta}{2}$ and $0 < t < 2 - \sqrt{3}$

Free Streamline for $\beta = \frac{2\pi}{3}$

$$z = \frac{1}{\pi} \left(2 \ln \left(\frac{1 - \sqrt{\lambda}}{1 + \sqrt{\lambda}} \right) + \ln \left(\frac{\lambda - \sqrt{\lambda} + 1}{\lambda + \sqrt{\lambda} + 1} \right) + 2\sqrt{3} \arctan \left(\frac{\sqrt{3\lambda}}{\lambda - 1} \right) \right) \quad (2.67)$$

On the free streamlines, $\lambda = e^{-i\theta}$, $0 < \theta < \frac{2\pi}{3}$. thus

$$\begin{aligned}
x &= -\sqrt{3} - \frac{1}{\pi} \left(\ln \left(\frac{-t^2 + 3}{-3t^2 + 1} \right) - 2 \ln t \right) \\
y &= 1 - \frac{\sqrt{3}}{\pi} \ln \left(\frac{(\sqrt{3} - t)(\sqrt{3} - 3t)}{(\sqrt{3} + t)(\sqrt{3} + 3t)} \right)
\end{aligned} \quad (2.68)$$

where $t = \tan \frac{\theta}{4}$; $0 < t < \frac{\sqrt{3}}{3}$

Free Streamline for $\beta = \frac{3\pi}{4}$

$$z = \frac{1}{\pi} \left(2 \ln \left(\frac{1 - \lambda^{\frac{1}{3}}}{1 + \lambda^{\frac{1}{3}}} \right) - \sqrt{2} \ln \left(\frac{\lambda^{\frac{2}{3}} + \lambda^{\frac{1}{3}}\sqrt{2} + 1}{\lambda^{\frac{2}{3}} - \lambda^{\frac{1}{3}}\sqrt{2} + 1} \right) - 4 \arctan(\lambda^{\frac{1}{3}}) + 2\sqrt{2} \arctan \left(\frac{\lambda^{\frac{1}{3}}\sqrt{2}}{\lambda^{\frac{2}{3}} - 1} \right) \right)$$

On the free streamlines, $\lambda = e^{-i\theta}$, $0 < \theta < \frac{3\pi}{4}$. thus

$$\begin{aligned}
x &= -1 - \sqrt{2} - \frac{2\sqrt{2}\ln(\sqrt{2} - 1)}{\pi} - \frac{1}{\pi} \left(\sqrt{2} \ln \left(\frac{(\sqrt{2} + 1)^2 - t^2}{(\sqrt{2} - 1)^2 - t^2} \right) - 2 \ln t \right) \\
y &= 1 - \frac{1}{\pi} \left(\sqrt{2} \ln \left(\frac{(\sqrt{2} - t)^2 - 1}{(\sqrt{2} + t)^2 - 1} \right) + 2 \ln \left(\frac{1 - t}{1 + t} \right) \right)
\end{aligned}$$

where $t = \tan \frac{\theta}{6}$; $0 < t < \sqrt{2} - 1$

Free Streamline for $\beta = \frac{5\pi}{6}$

$$z = \frac{1}{\pi} \left(2 \ln \left(\frac{1-\lambda^{\frac{1}{5}}}{1+\lambda^{\frac{1}{5}}} \right) + \sqrt{3} \ln \left(\frac{\lambda^{\frac{2}{5}} - \sqrt{3}\lambda^{\frac{1}{5}} + 1}{\lambda^{\frac{2}{5}} + \sqrt{3}\lambda^{\frac{1}{5}} + 1} \right) + \ln \left(\frac{\lambda^{\frac{2}{5}} - \lambda^{\frac{1}{5}} + 1}{\lambda^{\frac{2}{5}} + \lambda^{\frac{1}{5}} + 1} \right) + 2\sqrt{3} \arctan \left(\frac{\sqrt{3}\lambda^{\frac{1}{5}}}{\lambda^{\frac{2}{5}} - 1} \right) \right. \\ \left. + 2 \arctan \left(\frac{\lambda^{\frac{1}{5}}}{\lambda^{\frac{2}{5}} - 1} \right) - 4 \arctan \left(\lambda^{\frac{1}{5}} \right) \right)$$

On the free streamlines, $\lambda = e^{-i\theta}$, $0 < \theta < \frac{5\pi}{6}$. thus

$$x = -\sqrt{3} - 2 - \frac{2\sqrt{3} \ln(2 - \sqrt{3})}{\pi} - \frac{1}{\pi} \left(\sqrt{3} \ln \left(\frac{(2 + \sqrt{3})^2 - t^2}{(-2 + \sqrt{3})^2 - t^2} \right) + \ln \left(\frac{-t^2 + 3}{-3t^2 + 1} \right) - 2 \ln t \right) \\ y = 1 - \frac{1}{\pi} \left(\sqrt{3} \ln \left(\frac{(\sqrt{3} - t)(\sqrt{3} - 3t)}{(\sqrt{3} + t)(\sqrt{3} + 3t)} \right) + \ln \left(\frac{3 - (-t + 2)^2}{3 - (t + 2)^2} \right) + 2 \ln \left(\frac{1 - t}{1 + t} \right) \right)$$

where $t = \tan \frac{\theta}{10}$, $0 < t < 2 - \sqrt{3}$

The resulting free-streaming profiles for $\beta = \frac{\pi}{3}$, $\beta = \frac{\pi}{2}$ and $\beta = \frac{2\pi}{3}$ are shown in figure 2.4, figure 2.5 and figure 2.6 Respectively.

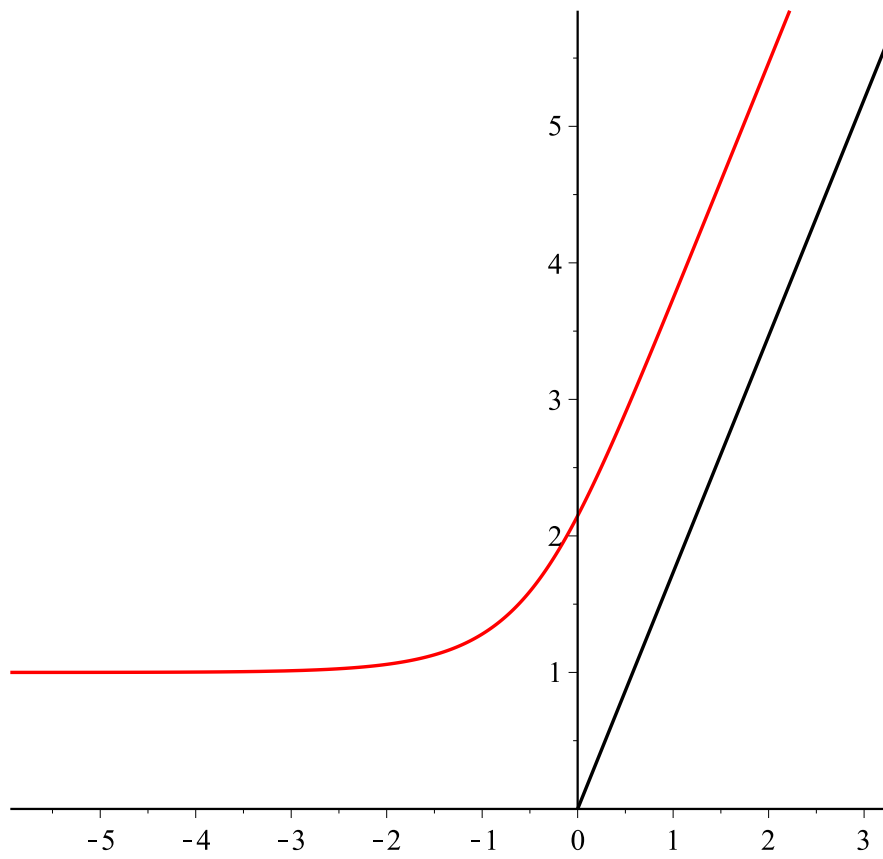


Figure 2.4: The free surface shape for $\frac{\pi}{3}$

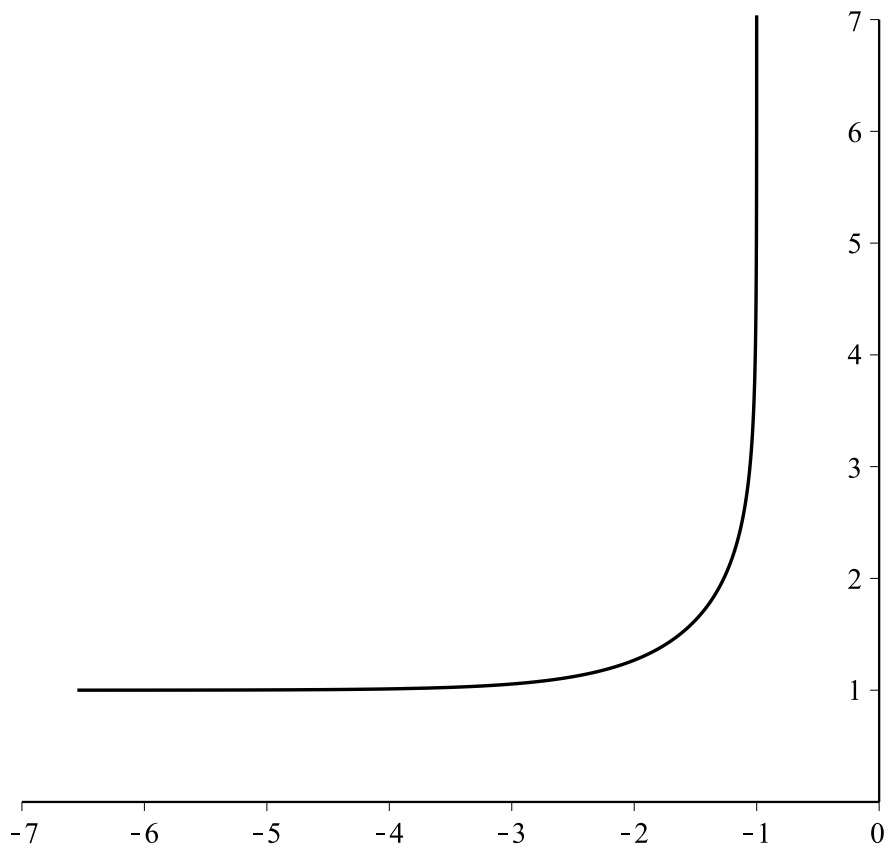


Figure 2.5: The free surface shape for $\frac{\pi}{2}$

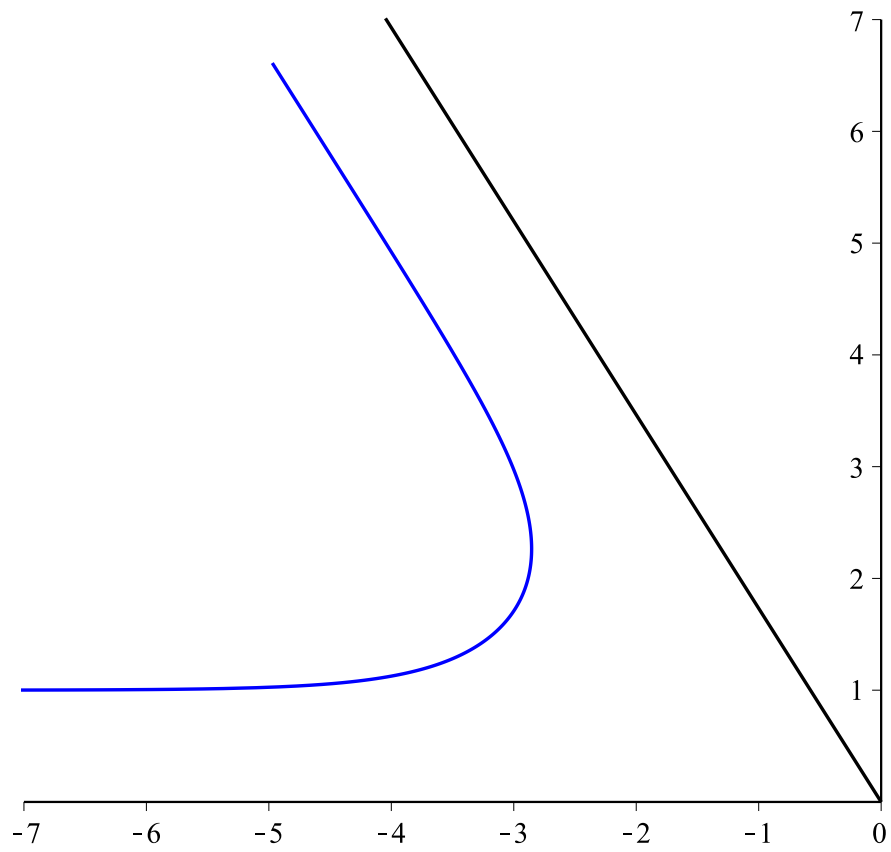


Figure 2.6: The free surface shape for $\frac{2\pi}{3}$

Conclusion

Throughout all the presented figures, we observe that the results obtained using the hodograph method agree with the results of M.J. Cooker [11], as well as with the results obtained using the Hilbert transform and the generalized Schwarz-Christoffel transformation technique by Weidong Peng and David F Parker [28] in the case where the surface tension effect is neglected. In this work, The hodograph method has proven to be a reliable and efficient technique for solving two-dimensional steady flow problems. It has been shown to produce accurate results in cases where other methods, such as the Hilbert transform and the generalized Schwarz-Christoffel transformation, have been used. One of the advantages of the hodograph method is that it reduces the problem to a free linear boundary problem, which simplifies the solution process. Additionally, the method only requires finding the solution on the free surface, rather than solving the problem in the entire domain. Overall, the hodograph method is a valuable tool for solving two-dimensional steady flow problems and has the potential to be applied to other fluid dynamics problems.

Chapter 3

Surface tension effects on jet flow past an infinite wedge

We are studying the problem presented in the second chapter, considering the effect of surface tension. We are using a numerical solution to determine the shape of the free surface, and employing the boundary integration method. This problem was previously studied by A Merzougui, H Mekias, and F Guechi [25] using the series truncation method. He found the shape of the free surface under two conditions: when the angle of the wedge changes and the surface tension is constant, and when the surface tension changes and the angle of the wedge is constant. The following parameters will be used to describe the flow, as we shall see: the Weber number is , represented by

$$\alpha = \frac{\rho U^2 H}{T} \tag{3.1}$$

, where ρ is the density of the fluid, U is the velocity of the flow, H is a characteristic length scale of the problem, and T is the surface tension coefficient. The value of α represents the ratio of the inertial forces to the surface tension forces and is a measure of the relative importance of surface tension in the problem. When α is small, surface tension is dominant, while when α is large, inertia dominates. In our problem, we will use the

numerical method of the differential integral equation to solve for the free surface shape under the effect of surface tension. The boundary integral equation method (BIEM) is a numerical technique used to solve partial differential equations (PDEs) in the context of boundary value problems. BIEM is commonly used to solve the fluid flow problems. The BIEM approach involves dividing the boundary of the domain into a set of discrete boundary elements. These boundary elements are then used to approximate the solution at each point on the boundary of the fluid domain. The BIEM method simplifies the problem of solving partial differential equations for the entire fluid domain by reducing it to solving a set of algebraic equations on the boundary of the domain. This approach can significantly reduce computational costs compared to other numerical methods, such as the finite element method, which requires the discretization of the entire fluid domain.

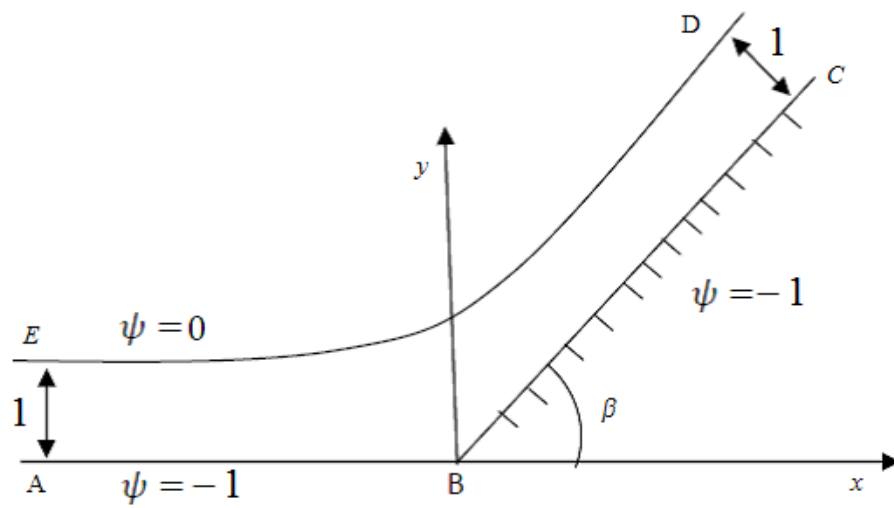


Figure 3.1: z-plane

3.1 Formulation of the problem

According to the second chapter, where ϕ is the velocity potential, we have Laplace's equation in the flow domain:

$$\Delta\phi = 0 \quad (3.2)$$

and the corresponding boundary conditions. The kinematic conditions on the solid walls AB and BC

$$\frac{\partial\phi}{\partial y} = 0 \quad (3.3)$$

and

$$\frac{\partial\phi}{\partial y} = \frac{\partial\phi}{\partial x} \tan(\beta) \quad (3.4)$$

On the free surface ED , applying Bernoulli's equation yields the dynamic boundary condition:

$$\frac{1}{2}q^2 + \frac{p}{\rho} = \frac{1}{2}U^2 + \frac{p_0}{\rho} \quad (3.5)$$

Here, ρ represents the constant density of the fluid p is the pressure in the fluid at the surface, p_0 is the atmospheric pressure, We have that because of surface tension, there is a differential in pressure along the free surface

$$p - p_0 = kT \quad (3.6)$$

The symbol T denotes the coefficient of surface tension, while k represents the curvature. Substituting equations 3.1 and 3.6 into equation 3.5, we obtain

$$\left(\frac{\partial\phi}{\partial x}\right)^2 + \left(\frac{\partial\phi}{\partial y}\right)^2 - \frac{2}{\alpha}k = 1 \quad (3.7)$$

3.2 Conformal mapping

The complex potential $f(z) = \phi + i\psi$ is an analytic function of the complex variable $z = x + iy$ (except at singular points). Here, ψ is the stream function that satisfies

Laplace's equation. This is because the velocity potential ϕ satisfies (3.2), as well. We can set $\psi = 0$ on the free surface and $\psi = -1$ on the base of the flow. By doing so, the kinematic condition (3.3) and (3.4) are satisfied. We are also free to choose a value for ϕ at a specific location along the base of the channel. For flow over an inclined wall, we choose $\phi = 0$ at the wedge apex. A schematic of the mapping from the z -plane to the w -plane is shown in Figure (3.1) and (3.2) the change is then used to map the w -plane to the ζ -plane.

$$\zeta = \xi + i\eta = e^{-\pi f} \quad (3.8)$$

According to , the free surface DE maps to the positive real axis ($\eta = 0, \xi > 0$), while the base of the channel ABC maps to the negative real axis ($\eta = 0, \xi < 0$) Figure(3.3). Since the position of B in the ζ -plane and the value of the velocity potential at point B are both unknown at the outset, we denote this spot as $\xi = -b, \eta = 0$. The flow region fills the top half of the ζ -plane, and the uniform flow far upstream AE is defined by the limit $|\zeta| \rightarrow +\infty$ ($\eta > 0$). Be aware that all channel flows over the walls, are covered by the mapping (3.8).

To fit the f -plane, the kinetic boundary conditions (3.3) and (3.4) were modified as follows on $\psi = -1$

$$\frac{\partial \phi}{\partial y} = 0, \quad \phi < \phi_B, \quad (3.9)$$

and

$$\frac{\partial \phi}{\partial y} = \frac{\partial \phi}{\partial x} \tan(\beta), \quad \phi_B < \phi < \infty, \quad (3.10)$$

On $\psi = 0$

We write the complex speed with the new variables τ and θ by:

$$\frac{df}{dz} = u - iv = e^{\tau - i\theta} \quad (3.11)$$

From 3.11 we find

$$u^2 + v^2 = e^{2\tau} (\cos^2 \theta + \sin^2 \theta) = e^{2\tau} \quad (3.12)$$

It is known that on the free surface

$$K = \frac{1}{R} = \frac{\partial \theta}{\partial s} = \left(\frac{\partial \theta}{\partial \phi} \frac{\partial \phi}{\partial s} + \frac{\partial \theta}{\partial \psi} \frac{\partial \psi}{\partial s} \right), \quad (3.13)$$

where R radius of the curvature and s is the curved free surface.

Since $\psi = 0$ along a streamline, $\frac{\partial \phi}{\partial s}$. Furthermore

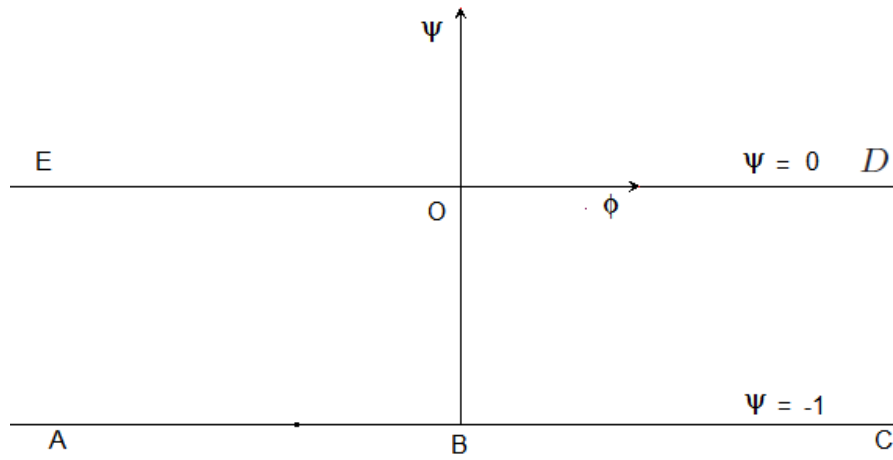
$$\frac{\partial \phi}{\partial s} = e^\tau. \quad (3.14)$$

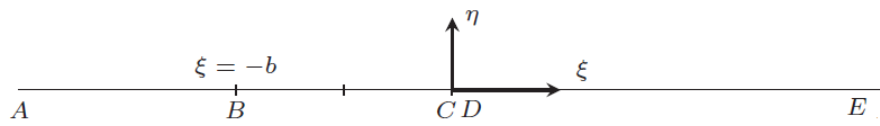
Therefore (3.13) can be simplified to

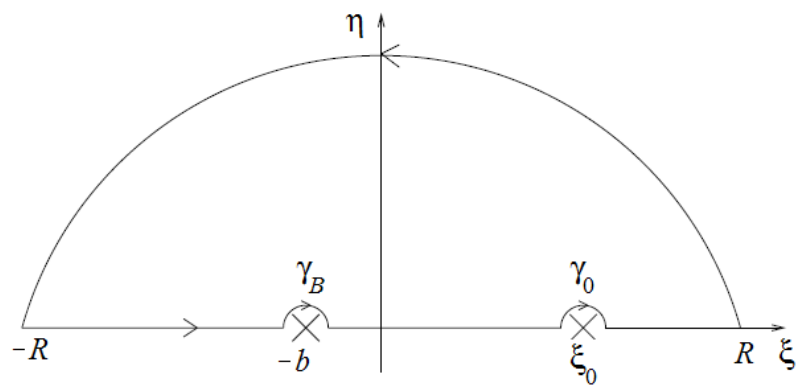
$$K = e^\tau \frac{\partial \theta}{\partial \phi}. \quad (3.15)$$

As a result, the Bernoulli equation (3.5) in non-dimensional variables on the streamline $\psi = 0$ is written:

$$\frac{1}{2} e^{2\tau} - \frac{e^\tau}{\alpha} \frac{\partial \theta}{\partial \phi} = \frac{1}{2}, \quad -\infty < \phi < \infty, \quad (3.16)$$

Figure 3.2: f -plane

Figure 3.3: ζ -plane

Figure 3.4: ζ -plane

3.3 Boundary integral approach

We next consider the complex velocity

$$\frac{df}{dz} = qe^{-i\theta} \quad (3.17)$$

in which q is the fluid speed and θ is the angle that the fluid velocity vector makes with the positive x axis

and, as such,

$$\Omega = \ln \left(\frac{df}{dz} \right) = \ln(q) - i\theta = \tau - i\theta \quad (3.18)$$

is an analytical function of ζ . Applying Cauchy's integral formula to Ω and assuming that the contour is made up of a semi-circle with a center at $\zeta = 0$ and a radius R , see figure 3.4 we can obtain an integral equation see Scott Tooley ([34]). The imaginary portion of the limit $R \rightarrow +\infty$ gives

$$\tau(\xi_0) = \frac{1}{\pi} \int_{-\infty}^{+\infty} \frac{\theta(\xi)}{\xi - \xi_0} d\xi \quad (3.19)$$

where here q and θ are real quantities on the boundary of the flow domain. The integral in (3.19) is of Cauchy Principal Value type.

For flow over an inclined wall, as depicted in Figure (3.1), the function $\theta(\xi)$ for $\xi < 0$ describes the angle of the wall. Since the sloped face of the wall maps to $-b < \xi < 0$, we have as an input to the problem

$$\theta(\xi) = \begin{cases} 0 & \xi < -b \\ \beta & -b < \xi < 0 \end{cases} \quad (3.20)$$

The boundary conditions (3.20), can be used to simplify (3.19). First, the integral is separated into three parts to give

$$\frac{1}{\pi} \int_{-\infty}^{\infty} \frac{\theta(\xi)}{\xi - \xi_0} d\xi = \frac{1}{\pi} \left(\int_{-\infty}^{-b} \frac{\theta(\xi)}{\xi - \xi_0} d\xi + \int_{-b}^0 \frac{\theta(\xi)}{\xi - \xi_0} d\xi + \int_0^{\infty} \frac{\theta(\xi)}{\xi - \xi_0} d\xi \right) \quad (3.21)$$

$$= \frac{1}{\pi} \left(\int_{-b}^0 \frac{\beta}{\xi - \xi_0} d\xi + \int_0^{\infty} \frac{\theta(\xi)}{\xi - \xi_0} d\xi \right) \quad (3.22)$$

therefore, (3.19) simplifies to

$$\tau(\xi_0) = -\frac{\beta}{\pi} \ln \frac{\xi_0 + b}{\xi_0} + \frac{1}{\pi} \int_0^{+\infty} \frac{\theta(\xi)}{\xi - \xi_0} d\xi, \quad \xi_0 > 0 \quad (3.23)$$

This equation holds along the free surface $\psi = 0$ and so using (3.8), results in

$$\xi + i\eta = e^{-\pi f} = e^{-\pi(\phi + i\psi)} = e^{-\pi\phi} \quad (3.24)$$

from 3.24 we find

$$\xi = e^{-\pi\phi} \quad (3.25)$$

Substituting (3.25) into (3.23) yields

$$\tau'(e^{-\pi\phi_0}) = -\frac{\beta}{\pi} \ln \left(\frac{e^{-\pi\phi_0} + b}{e^{-\pi\phi_0}} \right) + \int_{-\infty}^{\infty} \frac{e^{-\pi\phi} \theta'(\phi)}{e^{-\pi\phi} - e^{-\pi\phi_0}} d\phi \quad (3.26)$$

where $\xi_0 = e^{-\pi\phi_0}$, $\theta'(\phi) = \theta(e^{-\pi\phi})$, and $\tau'(\phi_0) = \tau(e^{-\pi\phi_0})$. On a free surface ED , the

Bernoulli equation(3.16) is satisfied

$$\frac{1}{2} e^{2\tau'} - \frac{e^{\tau'}}{\alpha} \frac{\partial \theta'}{\partial \phi} = \frac{1}{2}, \quad -\infty < \phi < \infty \quad (3.27)$$

Substituting (3.26) into (3.27) we get a nonlinear differential integral equation Unknown function θ' .

3.3.1 Numerical procedure

The points of the free surface in the complex potential plane f are represented by $\psi = 0$ and $-\infty < \phi < +\infty$: By discretizing the interval $] -a; a[$ at N points, where $a > 0$ is a large enough number.

$$\phi_i = \left((i-1) - \frac{N-1}{2} \right) h, \quad i = 1, \dots, N$$

where h is the step length, Value can be approximated if the integral (3.26) is evaluated by the trapezoidal rule, with a summation over ϕ_i such that ϕ_0 is the midpoint of one sub-interval, defined as follows

$$\phi_i^m = \frac{\phi_i + \phi_{i+1}}{2}, \quad i = 1, \dots, N-1 \quad (3.28)$$

Firstly, (3.26) is rewritten as

$$\tau_i^m = \sum_{j=1}^N \frac{\theta_j e^{-\pi\phi_j} w_j h}{e^{-\pi\phi_j} - e^{-\pi\phi_i^m}} d\phi - \frac{\beta}{\pi} \ln\left(\frac{e^{-\pi\phi_i^m} + b}{e^{-\pi\phi_i^m}}\right), \quad i = 1, \dots, N-1 \quad (3.29)$$

where $\tau_i^m = \tau'(\phi_i^m)$ and $\theta_j = \theta'(\phi_j)$

$$w_j = \begin{cases} \frac{1}{2} & j = 1, N \\ 1 & \text{otherwise} \end{cases}$$

The derivative $\frac{\partial\theta}{\partial\phi}$ at the mesh points (3.28) is approximated by a finite difference, given by

$$\frac{\partial\theta}{\partial\phi} \approx \frac{\theta_{i+1} - \theta_i}{h} \quad i = 1, \dots, N-1 \quad (3.30)$$

By substituting (3.29) and (3.30) into (3.27), and evaluating them at grid points (3.28), we obtain

$$\frac{1}{2} e^{2\tau_i^m} - \frac{e^{\tau_i^m}}{\alpha} \frac{(\theta_{i+1} - \theta_i)}{h} - \frac{1}{2} = 0, \quad i = 1, \dots, N-1 \quad (3.31)$$

A system of $N-1$ nonlinear equations in $N+1$ unknowns is obtained. These unknowns are θ_i for $i = 1, \dots, N$ and b . that another tow equations are needed to complete the system. These equations can be constructed by fixing a value to b , and the condition that there are no waves as $|y| \rightarrow +\infty$ is imposed by requiring $\theta_{N-1} = \theta_N$. To solve this system(3.31) we use Newton's method.

3.3.2 Cartesian coordinates of the free surface

From the relation 3.11 we find

$$\frac{dz}{df} = e^{-\tau+i\theta} \quad (3.32)$$

So

$$dz = e^{-\tau+i\theta}(d\phi + id\psi) \quad (3.33)$$

as $d\psi = 0$ on the free surface, it comes:

$$\begin{cases} \frac{dx}{d\phi} = e^{-\tau} \cos \theta \\ \frac{dy}{d\phi} = e^{-\tau} \sin \theta \end{cases}$$

For approximating the value of the derivatives at ϕ_i^m for $i = 1, 2, \dots, N - 1$

a central difference can be used to give the following recursive relations

$$\begin{cases} y_1 = 1 \\ y_{i+1} = y_i + he^{\tau_i^m} \sin \theta_i, \quad i = 1, \dots, N - 1 \end{cases}$$

and

$$\begin{cases} x_1 = \text{quite large} \\ x_{i+1} = x_i + he^{\tau_i^m} \cos \theta_i, \quad i = 1, \dots, N - 1 \end{cases}$$

3.3.3 Free surface profiles

The parameters chosen to generate such solutions were $b = 1$ and α . Figures 3.5 and 3.6 represent the comparison between the approximate solution and the exact solution obtained in the second chapter, where $\beta = \frac{\pi}{6}$ and $\frac{\pi}{2}$, respectively, and $\alpha \rightarrow +\infty$, meaning that $T = 0$ for $N = 100$ and $h = 0.1$. Figures 3.7, 3.8 and 3.9 The free surface is represented in the following cases:

$$\beta = \frac{2\pi}{3}, \alpha = 1, 4, 10 \text{ and } \alpha \rightarrow +\infty$$

$$\beta = \frac{\pi}{2}, \alpha = 0.5, 2, 20 \text{ and } \alpha \rightarrow +\infty$$

$$\beta = \frac{\pi}{3}, \alpha = 0.5, 2, 10 \text{ and } \alpha \rightarrow +\infty$$

for $N = 200$ and $h = 0.1$.

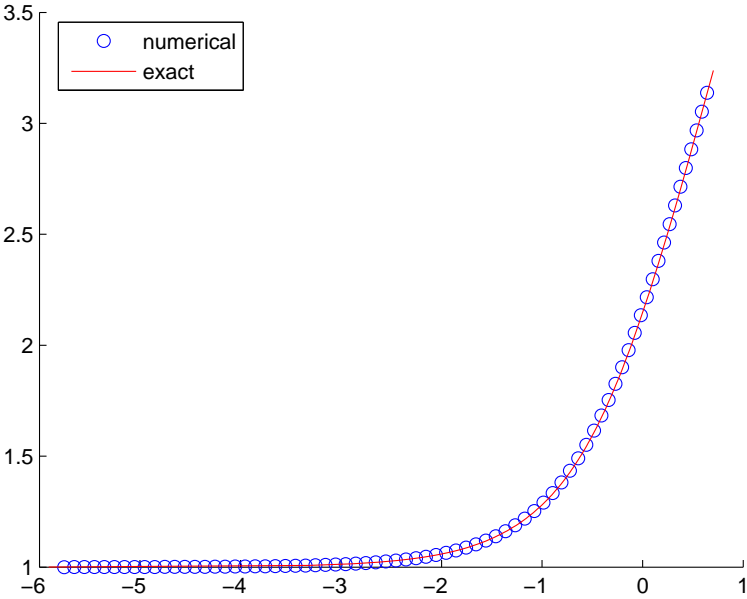


Figure 3.5: Comparison of the analytical solution and the numerical solution for $\frac{\pi}{6}$

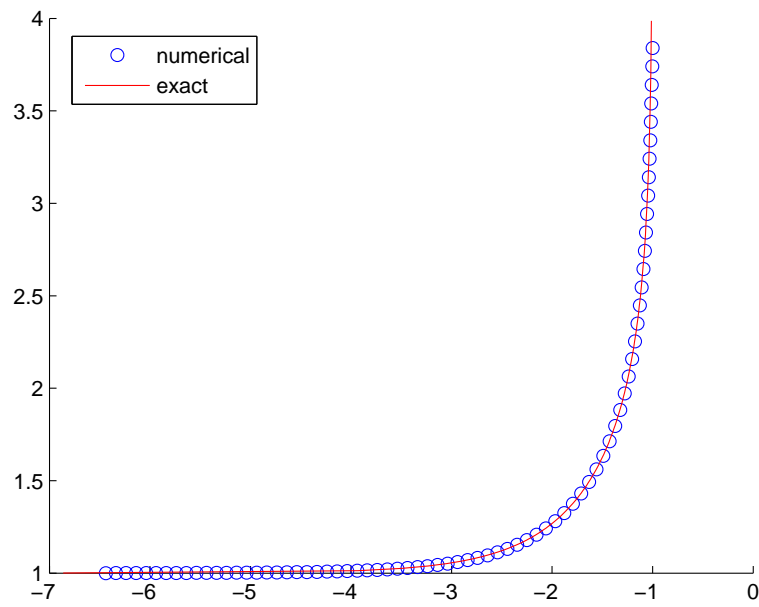


Figure 3.6: Comparison of the analytical solution and the numerical solution for $\frac{\pi}{2}$

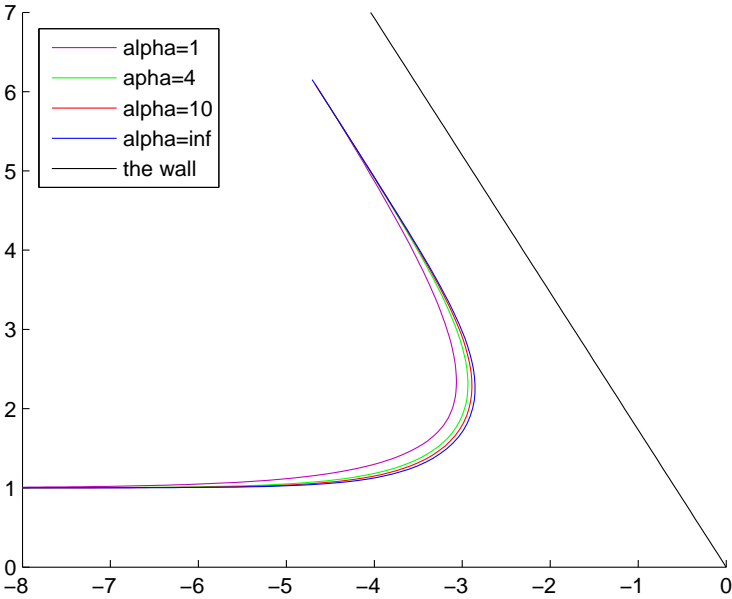


Figure 3.7: Free streamline shapes for $\frac{2\pi}{3}$ and various Weber numbers α

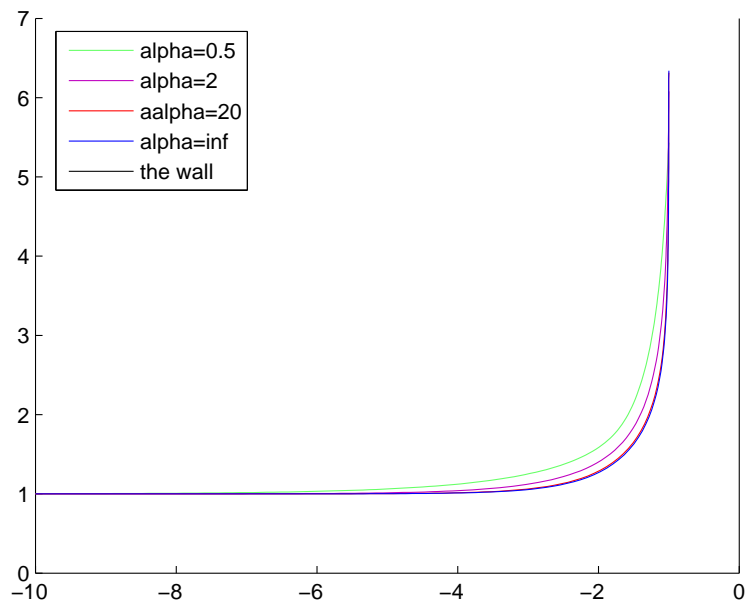


Figure 3.8: Free streamline shapes for $\frac{\pi}{2}$ and various Weber numbers α

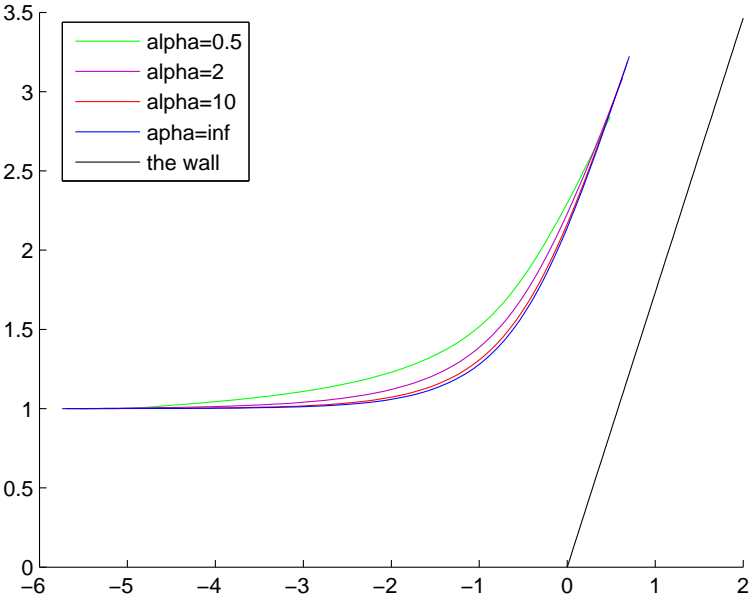


Figure 3.9: Free streamline shapes for $\frac{\pi}{3}$ and various Weber numbers α

Chapter 4

Nonlinear Free Surface Flow past a Wedge in Channel

In this work, the two-dimensional problem of irrotational flow past a wedge located in the center of the channel is considered. Assuming that the fluid is incompressible and non-viscous, the influence of gravity is ignored but the surface tension is considered. The problem which is characterized by the nonlinear boundary conditions on the free surface of the unknown equation is solved numerically by the series truncation technique. The results show that for all given wedge configurations, there is a critical value for the Weber number, for which there is no solution for every Weber number value smaller than this. In addition, the obtained results extend the work done by Gasmi and Mekias [14].

4.1 Introduction

In some physical phenomena, potential free surface flows of fluid past an obstacle can be observed, and due to its importance, it becomes the subject of more research. In this paper the steady two-dimensional irrotational flow of an incompressible and inviscid fluid past a wedge located in the center of a channel with a width of H_0 is considered. The effect of gravity is ignored, but we take into account the surface tension. Far upstream, the flow is

uniform and the speed is U_0 . Due to the existence of the wedge, the flow is divided into two parts, both of which extend to infinity with depths H and H' and with a constant velocities U and U' , respectively, see figure 4.1 For each value of the wedge angle, the problem is characterized by the three parameters, the two angles γ and γ' at the separations points between the wedge walls and the two free streamlines and the Weber number α defined by the following formula:

$$\alpha = \frac{\rho U^2 L}{T}, \quad (4.1)$$

where T is the surface tension and ρ is the density of the fluid. When the influence of surface tension T and the gravity effects are neglected, the mathematical solution can be obtained exactly by hodograph transformation, for example see Birkhof and Zarantonello [6] and Batchelor [5]. Under the same conditions, Dormiani, Bruch and Sloss [13] used the Schwarz alternate procedure to solve the problem of flow past truncated convex shaped profiles between walls in logarithmic plane. Gasmi and Mekias [[14],[18]], Bounif and Gasmi [9], Gasmi [[16], [15]], Gasmi and Amara [3], studied the problems of flow over an obstruction in a channel. Asavanant and Vanden-Breock [4] Vanden-Breock [36] and Naghdi and Vangsrnpigoon [27] have investigated the problem of flow under gate and a jet flow in the case when the surface tension effects are neglected and considering the effect of gravity. In the present work, we solved the fully nonlinear problem numerically and the mesh points were only on the free surface. For each value of the wedge angle, we found that there is a value of the Weber number α^* such that there exists a unique solution, for all $\alpha \geq \alpha^*$. If $\alpha < \alpha^*$ the numerical scheme diverges, in the particular case when the wedge angle is equal to $\beta = \frac{\pi}{2}$. In this work we extend the calculations of Gasmi and Mekias [2]. The problem is formulated in section 2, the numerical procedure is described in section 3 and in section 4 we present some results and discussion. Finally, this work is concluded in section 5.

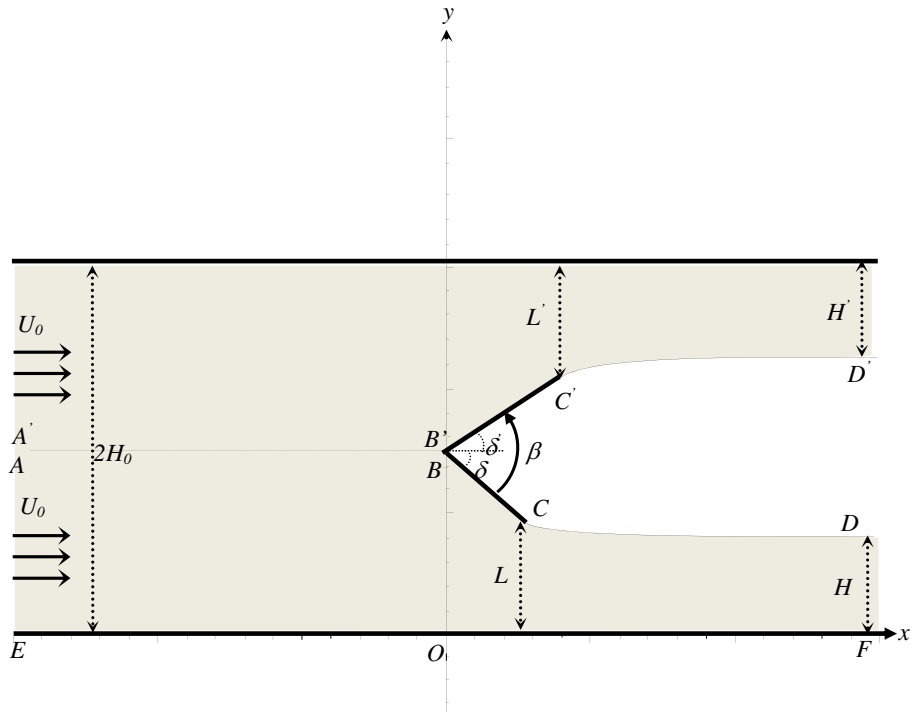


Figure 4.1: Sketch of the flow past a wedge and of the coordinates. The wedge angle is β , the width of the channel is $2H_0$ and the depth of the flow at infinity is $H + H'$. The x-axis is along the streamline EOF and the y vertically through the point.

4.2 Formulation of the problem

Let us consider the steady two-dimensional potential flow of fluid past a wedge CBC' with an apex angle $\beta = \delta + \delta'$, which is placed in the center of channel of width $2H_0$ and infinitely length, see figure4.1 The flow is considered to be steady, inviscid and incompressible. Gravity effects is neglected but the surface tension forces are taken into account. We introduce Cartesian coordinates with the streamline EOF on the \bar{x} axis and the \bar{y} axis is vertically through the point B . Far upstream the flow is uniform with a constant velocity U_0 . Far downstream, we assume that the velocity approaches a constant U and the depth of the fluid tends to a constant $H + H'$. The dimensionless variables are defined by choosing U_0 as the unit velocity and H_0 as the unit length. We introduce the potential function ϕ and the stream function ψ . Without loss of generality we choose $\phi = 0$ at $(x, y) = (0, 0)$ and $\psi = 0$ on the streamline EOF . It follows from the choice of the dimensionless variables that $\psi = -\frac{1}{2}$ on the streamline $A'B'C'D'$ and $\psi = \frac{1}{2}$ on the streamline $ABCD$. In order to use the conformal mapping techniques, we consider the flow in the complex plane $z = x + iy$ and the complex potential function $f = \phi + i\psi$. The half of the flow region considered in the $z - plane$ will be mapped via the potential function f onto the semi-infinite strip $(-\infty < \phi < +\infty, -\frac{1}{2} < \psi < \frac{1}{2})$, see figure4.2 We introduce the complex velocity $\zeta = u - iv = \frac{df}{dz}$.

Now our task is to solve the boundary value problem

$$\Delta\phi = 0, \quad \text{in the flow domain.} \quad (4.2)$$

The dynamic condition on the free surfaces CD and $C'D'$ is expressed by Bernoulli equation

$$\frac{1}{2}q^2 + \frac{p}{\rho} = \frac{1}{2}U^2 + \frac{p_0}{\rho}, \quad \text{on} \quad \psi = \pm\frac{1}{2}, \quad \phi > 0, \quad (4.3)$$

The other condition is kinematic along the solid and the free boundaries satisfying

$$\frac{\partial\phi}{\partial\eta} = 0, \quad \text{on the walls,} \quad (4.4)$$

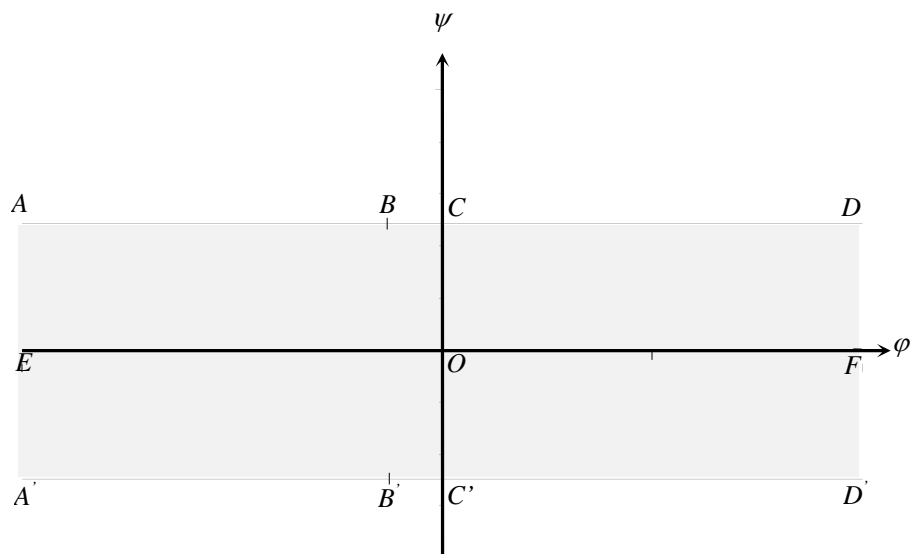


Figure 4.2: Flow configuration in the complex potential f -plane.

where η is the normal vector of the boundaries. In dimensionless variables (4.3) becomes:

$$\left(\frac{\partial\phi}{\partial x}\right)^2 + \left(\frac{\partial\phi}{\partial y}\right)^2 - \frac{2}{\alpha}K = 1, \quad \text{on} \quad \psi = \pm\frac{1}{2}, \quad \phi > 0. \quad (4.5)$$

Here K is the curvature of the free surface and α is the Weber number defined by (4.1) In order that the curvature will be well defined we introduce the function $\tau - i\theta$ as:

$$\zeta = u - iv = e^{\tau - i\theta}. \quad (4.6)$$

We use (4.6) to express (4.5) in terms of the complex variables τ and θ . The velocity terms, first, become

$$q^2 = u^2 + v^2 = e^{2\tau}(\cos^2\theta + \sin^2\theta) = e^{2\tau}. \quad (4.7)$$

Secondly, the curvature K of the streamline, in terms of θ , is

$$K = \frac{1}{R} = \frac{\partial\theta}{\partial s} = \left(\frac{\partial\theta}{\partial\phi}\frac{\partial\phi}{\partial s} + \frac{\partial\theta}{\partial\psi}\frac{\partial\psi}{\partial s}\right), \quad (4.8)$$

where R radius of the curvature and s is the curved free surface.

Since $\psi = \text{constant}$ along a streamline, $\frac{\partial\psi}{\partial s} = 0$. Furthermore

$$\frac{\partial\phi}{\partial s} = e^\tau. \quad (4.9)$$

Therefore (4.21) can be simplified to

$$K = e^\tau \frac{\partial\theta}{\partial\phi}. \quad (4.10)$$

Substituting (4.10) and (4.7) into (4.4), gives the final form of Bernoulli's equation that is needed for numerical calculation. This is

$$\frac{1}{2}e^{2\tau} - \frac{e^\tau}{\alpha}\frac{\partial\theta}{\partial\phi} = \frac{1}{2}, \quad \text{on} \quad \psi = \pm\frac{1}{2}, \quad \phi > 0, \quad (4.11)$$

The kinematic condition on $AB, A'B', BC$ and $B'C'$ can be expressed as:

$$\text{Im}(\zeta) = 0 \quad \text{on} \quad \psi = \pm\frac{1}{2} \quad \text{and} \quad -\infty < \phi < \phi_B \text{ (respectively, } \phi_{B'}). \quad (4.12)$$

$$\frac{\text{Im}(\zeta)}{\text{Re}(\zeta)} = \tan(\delta) \quad \text{on} \quad \psi = \frac{1}{2}, \quad \phi_B < \phi < \phi_C. \quad (4.13)$$

$$\frac{\text{Im}(\zeta)}{\text{Re}(\zeta)} = \tan(\delta') \quad \text{on} \quad \psi = -\frac{1}{2}, \quad \phi_{B'} < \phi < \phi_{C'}. \quad (4.14)$$

This completes the formulation of the problem of determining $\tau - i\theta$. For given values of α , β and H , this function must be analytic in the strip $-\frac{1}{2} < \psi < \frac{1}{2}$ and satisfy conditions (4.11), (4.12), (4.13) and (4.14).

4.3 Numerical procedure

Using the same scheme introduced by Vanden-broeck[36] and Gasmi and Mekias[[14],[16]], first we map the flow domain into the half of the unit disk in the complex t -plane by the transformation

$$f = \frac{1}{\pi} \log\left(\frac{2t}{1-t^2}\right). \quad (4.15)$$

The wall $A'B'$, $B'C'$, AB , BC goes onto the imaginary interval $(-i, i)$, the wall EOF onto the real interval $(0, 1)$ and the free surfaces CD and $C'D'$ onto the circumference (see figure 4.3). Since there are stagnation points at B and B' , and discontinuity in the derivative $\frac{\partial\theta}{\partial\phi}$ at the separation points C and C' must have zeros and poles at these points. Local analysis shows that appropriate zeros and singularities are

$$\zeta \sim (t^2 + b^2)^{\frac{\delta}{\pi}} \quad \text{as}, \quad t \longrightarrow ib. \quad (4.16)$$

$$\zeta \sim (t^2 + b'^2)^{\frac{\delta'}{\pi}} \quad \text{as}, \quad t \longrightarrow -ib'. \quad (4.17)$$

$$\zeta \sim (t^2 + 1)^{1-\frac{\gamma}{\pi}} \quad \text{as}, \quad t \longrightarrow i. \quad (4.18)$$

$$\zeta \sim (t^2 + 1)^{1-\frac{\gamma'}{\pi}} \quad \text{as}, \quad t \longrightarrow -i. \quad (4.19)$$

Here b and b' is the image of the corner B and B' in the t plane.

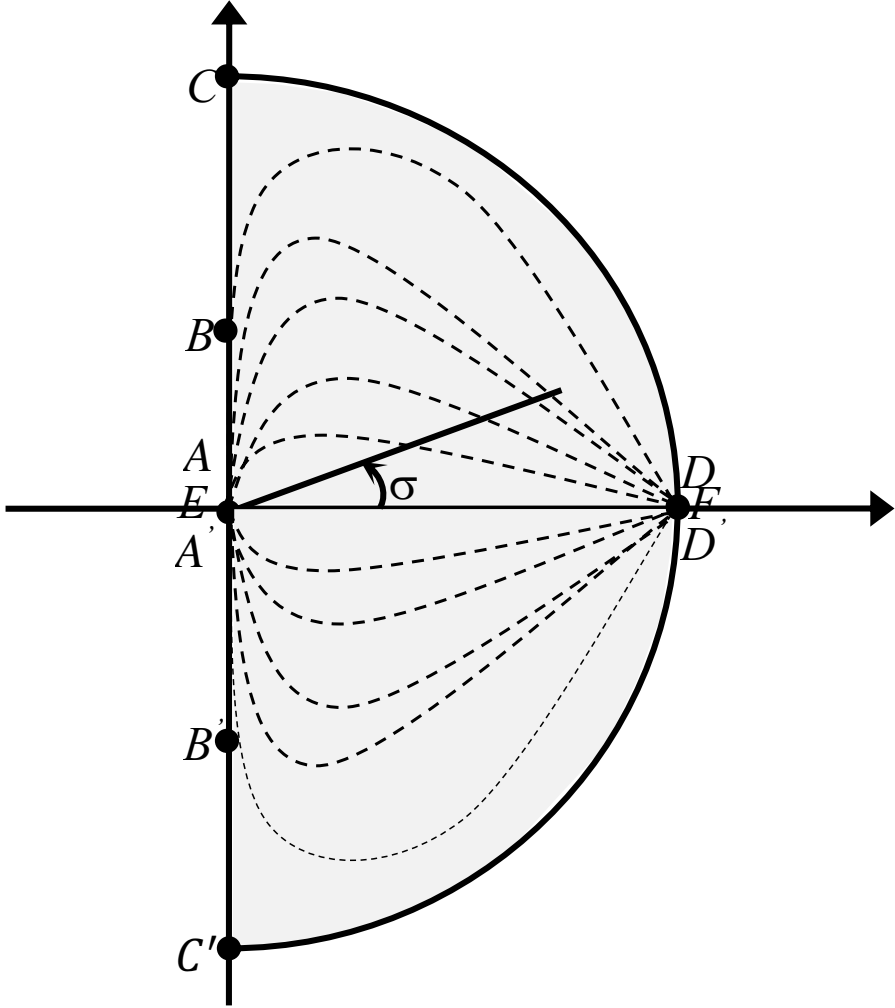


Figure 4.3: The image of the Flow in the t-plane.

Table 4.1: The positioning of the major points of the flow domain problem in the f-plane and the t-plane

Cartesian plane	f-plane	t-plane
A	$\psi = \frac{1}{2}, \phi = \phi_A = -\infty$	$t = 0$
B	$\psi = \frac{1}{2}, \phi = \phi_B < 0$	$t = ib$
C	$\psi = \frac{1}{2}, \phi = \phi_C = 0$	$t = i$
D	$\psi = \frac{1}{2}, \phi = \phi_D = +\infty$	$t = 1$
A'	$\psi = \frac{-1}{2}, \phi = \phi_{A'} = -\infty$	$t = 0$
B'	$\psi = \frac{-1}{2}, \phi = \phi_{B'} < 0$	$t = -ib'$
C'	$\psi = \frac{-1}{2}, \phi = \phi_{C'} = 0$	$t = -i$
D'	$\psi = \frac{-1}{2}, \phi = \phi_{D'} = +\infty$	$t = 1$
E	$\psi = 0, \phi = \phi_E = -\infty$	$t = 0$
O	$\psi = 0, \phi = \phi_O = 0$	$0 < t < 1$
F	$\psi = 0, \phi = \phi_F = +\infty$	$t = 1$

We define the function $\zeta(t)$ by the relation:

$$\zeta(t) = (t^2 + b^2)^{\frac{\delta}{\pi}} (t^2 + b'^2)^{\frac{\delta'}{\pi}} (t^2 + 1)^{1-\frac{\gamma}{\pi}} (t^2 + 1)^{1-\frac{\gamma'}{\pi}} e^{\Omega(t)}. \quad (4.20)$$

The ζ singularities are removed in (4.14) by the factors $(t^2 + b^2)^{\frac{\delta}{\pi}} (t^2 + b'^2)^{\frac{\delta'}{\pi}} (t^2 + 1)^{1-\frac{\gamma}{\pi}} (t^2 + 1)^{1-\frac{\gamma'}{\pi}}$. It follows that $\Omega(t)$ can be represented by Taylor expansion in power of t . Furthermore, the kinematic conditions 4.11, 4.12, 4.13 and 4.14 imply that the expansion for $\Omega(t)$ has real coefficients a_n and involves only even powers of t . Hence,

$$e^{\tau-i\theta} = \zeta(t) = (t^2 + b^2)^{\frac{\delta}{\pi}} (t^2 + b'^2)^{\frac{\delta'}{\pi}} (t^2 + 1)^{1-\frac{\gamma}{\pi}} (t^2 + 1)^{1-\frac{\gamma'}{\pi}} e^{\sum_{n=1}^{\infty} a_n t^{2n}}. \quad (4.21)$$

We use the notation $t = |t| e^{i\sigma}$ so that points on CD are given by $t = e^{i\sigma}$, $0 < \sigma < \frac{\pi}{2}$. Using (4.21) we rewrite (4.11) in the form:

$$e^{2\bar{\tau}} + \frac{\pi}{\alpha} e^{\bar{\tau}} \tan(\sigma) \frac{\partial \bar{\theta}}{\partial \sigma} = 1, \quad 0 < \sigma < \frac{\pi}{2}. \quad (4.22)$$

Here $\bar{\tau}(\sigma)$ and $\bar{\theta}(\sigma)$ denote the values of τ and θ on the free surface AB .

We solve the problem approximately by truncating the infinite series in (4.21) after N terms. We find the N coefficients a_n and the separation angle γ by collocation. Thus we introduce the N mesh points

$$\sigma_I = -\frac{\pi}{2(N+1)} \left(I - \frac{1}{2} \right), \quad I = 1, \dots, N+1 \quad (4.23)$$

Using (4.23) we obtain $\bar{\tau}(\sigma)]_{\sigma=\sigma_I}$, $[\bar{\theta}(\sigma)]_{\sigma=\sigma_I}$ and $[\frac{\partial \bar{\theta}}{\partial \sigma}]_{\sigma=\sigma_I}$ in terms of coefficients a_n and the separation angle γ . Thus, we obtain $(N+1)$ nonlinear algebraic equations of $(N+1)$ unknowns $(a_{n,n=1,\dots,N}, \gamma)$. for given values of the wedge angle β and Weber number α , this system of equations is solved by Newton's method.

Finally, the shape of the surface is obtained by integrating numerically the relation

$$\frac{\partial x}{\partial \sigma} = \frac{2}{\pi} \cot(\sigma) e^{\bar{\tau}} \cos(\bar{\theta}), \quad (4.24)$$

and

$$\frac{\partial y}{\partial \sigma} = \frac{2}{\pi} \cot(\sigma) e^{\bar{\tau}} \sin(\bar{\theta}). \quad (4.25)$$

4.4 Discussion of results

The numerical schemes of section 3 were used in the symmetrical case when $\delta = \delta'$ and $L = L'$ to compute solutions for different values of the wedge angle β and several values of the Weber number α . We found that the coefficients a_n decrease rapidly as n increases. Table 2 shows some of the coefficients of the series (4.21) and the corresponding Weber number for different values of β . Most of the calculations were done and presented with $N = 60$.

Table 4.2: Some values of the coefficients a_n of the series (4.21) for several values of the angle β , $b = b' = 0.5$ and different values of Weber number α

β	α	a_1	a_{20}	a_{40}	a_{60}
$\frac{\pi}{2}$	1.5	$1,445 \times 10^{-1}$	$1,325 \times 10^{-5}$	$2,503 \times 10^{-6}$	$1,377 \times 10^{-7}$
	10	$5,083 \times 10^{-2}$	$1,475 \times 10^{-5}$	$-4,983 \times 10^{-7}$	3.151×10^{-7}
	$\alpha \rightarrow \infty$	$1,554 \times 10^{-9}$	$3,726 \times 10^{-10}$	$2,839 \times 10^{-11}$	$-5,059 \times 10^{-14}$
π	1.5	$2,194 \times 10^{-1}$	$2,308 \times 10^{-6}$	$3,833 \times 10^{-7}$	$2,049 \times 10^{-8}$
	10	$1,158 \times 10^{-1}$	$9,558 \times 10^{-5}$	$2,078 \times 10^{-5}$	$1,270 \times 10^{-6}$
	$\alpha \rightarrow \infty$	$1,681 \times 10^{-1}$	$-4,704 \times 10^{-7}$	$-1,304 \times 10^{-12}$	$-4,195 \times 10^{-19}$
$\frac{3\pi}{2}$	1.5	$4,329 \times 10^{-1}$	$4,764 \times 10^{-5}$	$9,542 \times 10^{-6}$	$5,286 \times 10^{-7}$
	10	$1,521 \times 10^{-1}$	$4,516 \times 10^{-5}$	$-1,178 \times 10^{-6}$	$9,809 \times 10^{-7}$
	$\alpha \rightarrow \infty$	$4,846 \times 10^{-1}$	$6,931 \times 10^{-5}$	$-4,736 \times 10^{-6}$	$-1,057 \times 10^{-7}$

4.4.1 Flow with surface tension effect

When the effect of surface tension is included in the dynamical condition on the free surface, the numerical computational shows that there exists a critical value $\alpha = \alpha^*$ for each value of the wedge angle β and the number b , for which there is no solution for $\alpha < \alpha^*$ see table 3.

Table 4.3: Some values of the minimal Weber number for and different values of the wedge angle

$\beta = 2\delta = 2\delta'$	$\frac{\pi}{2}$	$\frac{2\pi}{3}$	π	$\frac{3\pi}{2}$	$\frac{4\pi}{3}$	$\frac{5\pi}{3}$
α^*	1,283	1,211	1,203	1,754	0,942	1,512

Accurate solutions for $\alpha \geq \alpha^*$ are obtained. As $b \rightarrow 1$ and for all wedge angle $0 \leq \beta \leq \frac{\pi}{2}$ we obtain the same results as Gasmi & Mekias[14] and our result also agree with the results of Ackerberg & Liu[2] for different Weber number $\alpha \geq \tilde{\alpha}$. These authors solved the problem via the finite difference method and the mesh point were throughout the fluid domain, they

could find solution for all $\alpha \geq \tilde{\alpha} = 6.801483$. In our procedure mesh points are only needed on the free surface and we computed solutions for $\alpha \leq \tilde{\alpha}$. For $\alpha > \tilde{\alpha}$ our results agree with theirs.

We note that the contraction coefficient C_c and the angle in the separation point increase as the Weber number α decreases. Numerical values of C_c versus $\frac{1}{\alpha}$ are presented in figure 4.4

In figure 4.5 we present values of the angle at the separation point between the wedge wall and the free streamlines γ versus $\frac{1}{\alpha}$. It is seen that numerical solutions exist for all $\alpha > \alpha^*$, whereas there is no solution for $\alpha < \alpha^*$. Typical profiles for various Weber numbers of the free surface are presented in figure 4.6 for $\beta = \frac{3\pi}{4}$, figure 4.7 for $\beta = \frac{\pi}{2}$ and figure 4.8 for $\beta = \frac{\pi}{4}$.

For $\beta = \frac{\pi}{2}$ our problem reduce to flow past a vertical flat plate in tunnel treated by Gasmi & Mekias[19]

4.4.2 Solution for large $\mathbf{T}(\alpha \rightarrow 0)$

When the surface tension is large. we have $\alpha \rightarrow 0$ and the profile of the jet approaches two horizontal straight lines, the contraction coefficient $C_c \rightarrow 1$ and the angle of separation $\gamma \rightarrow \pi + \delta$. For this limiting case, all boundaries are rectilinear, hence The solution is then

$$\begin{cases} \gamma = \pi + \frac{\beta}{2}, \\ a_n = 0, \quad n=1,2,\dots \end{cases} \quad (4.26)$$

Substituting equation 4.26 into equation 4.21, we obtain the following exact solution:

$$\tau(\sigma) - i\theta(\sigma) = \frac{\beta}{\pi} \log\left(\frac{b^2 + e^{2i\sigma}}{1 + e^{2i\sigma}}\right). \quad (4.27)$$

4.4.3 Flow without surface tension.

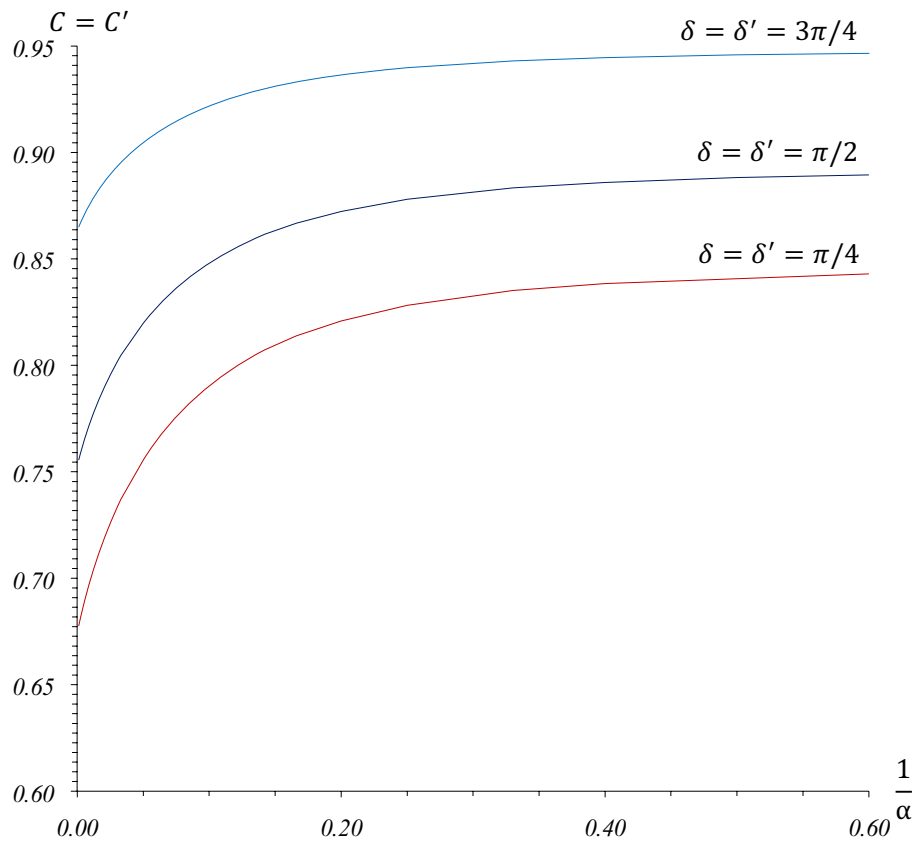
When the Weber number is very large $\alpha \geq 10^3$ and $b \rightarrow 1$ or the wedge angle β approaches zero whereas the flow reduces to the stream. As $b \rightarrow 0$ the problem reduces to the flow

under sluice gate of an inclined wall and for all inclination angles β , the exact analytical solutions can be computed via free stream line theory[5]. We computed numerically these solutions using the procedure described above and our results agree with the theoretical and experimental results given in Birkhoff, G., E.H. Zarantonello[6](see Figure 4.9). As $0 < b < 1$, the coefficients $a_n \sim 0$ and the angle $\gamma = 3.1415$, hence the solution is

$$\zeta(t) = (b^2 + t^2)^{\frac{\beta}{\pi}}. \quad (4.28)$$

wish is the classical Kirchhoff solution (Batchelor 1967)^[3].

for $\beta = \frac{\pi}{2}$ and $b = 0$ we obtain $C_c = 0.611$. The comparison of the free streamline shapes for $\beta = \frac{\pi}{2}$ and $\beta = \pi$ obtained using our methods with the theoretical exact solutions are presented in figure 4.10

Figure 4.4: Coefficients of contraction C and C' vs $\frac{1}{\alpha}$

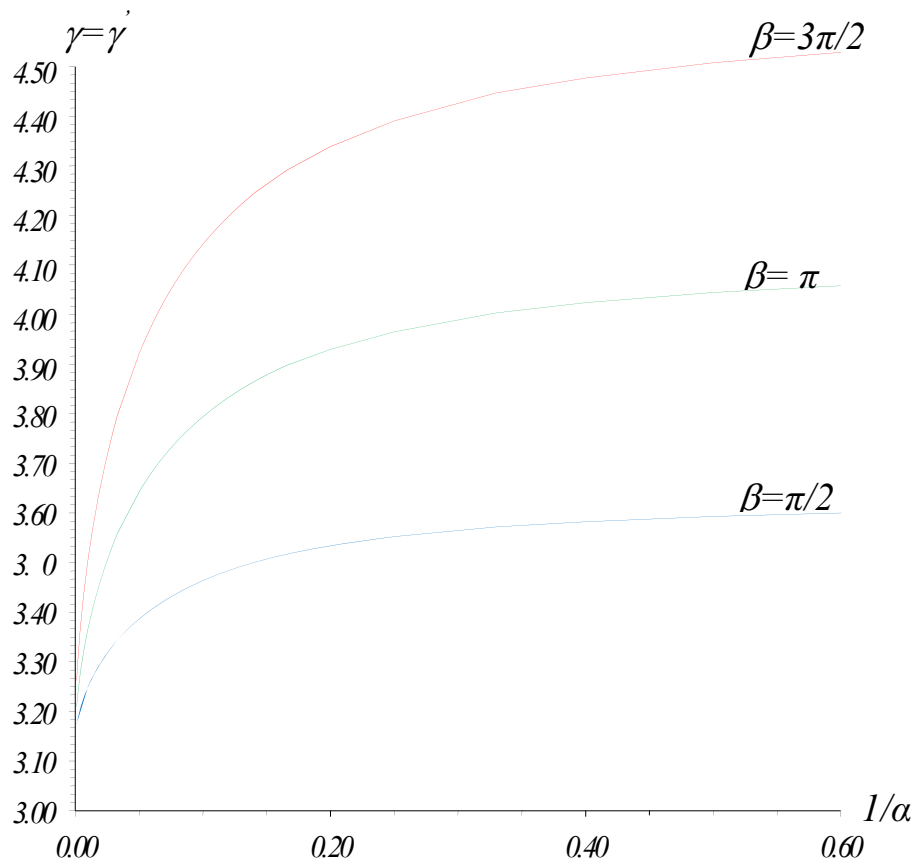


Figure 4.5: The angles of separation γ and γ' vs $\frac{1}{\alpha}$

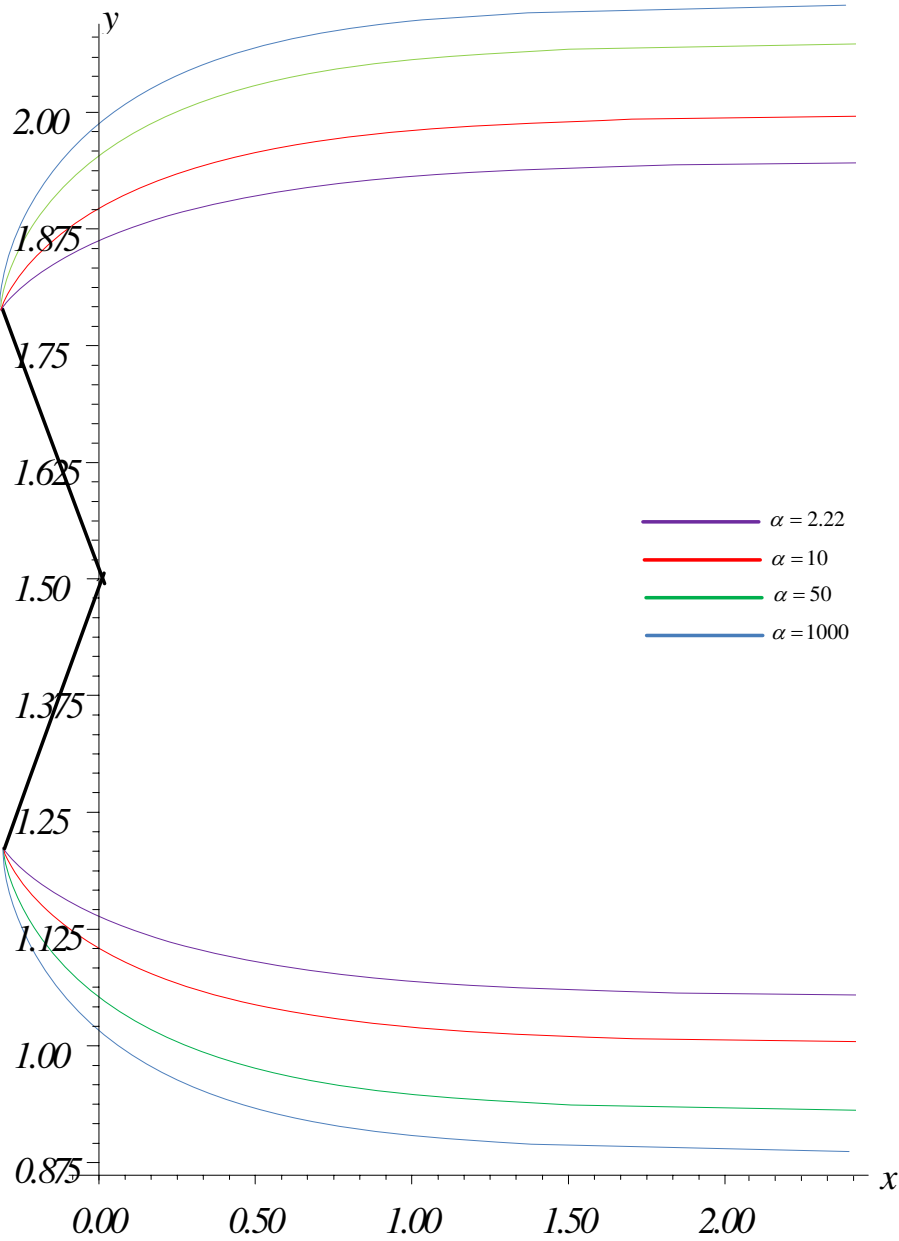


Figure 4.6: Computed free streamline shapes for $\beta = \frac{3\pi}{2}$, $b = b' = 0, 5$ and various Weber numbers

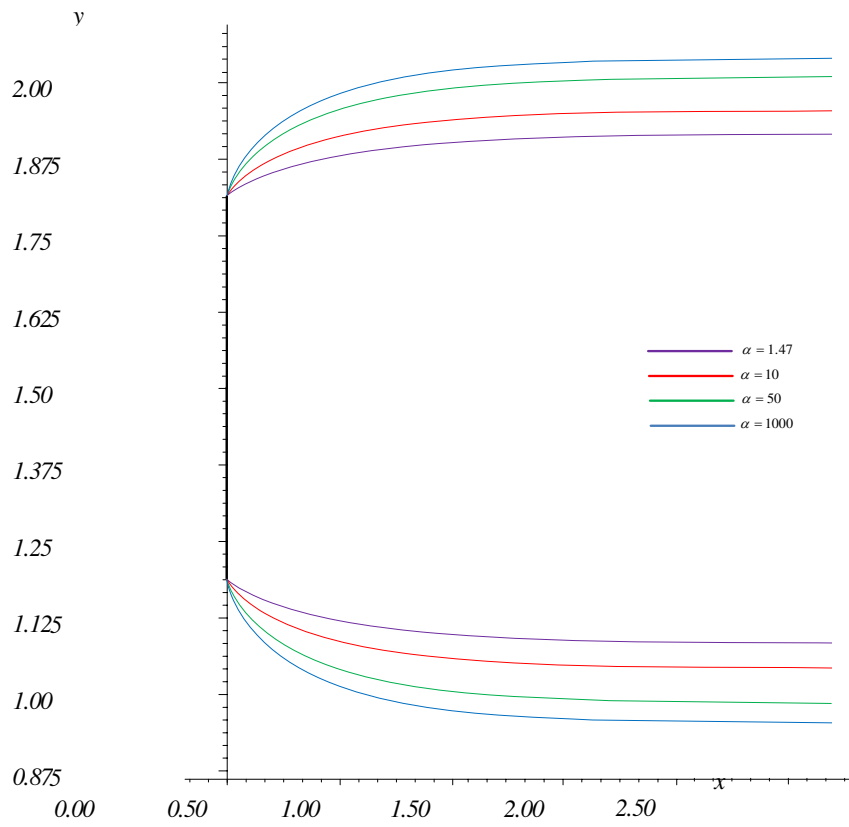


Figure 4.7: Computed free streamline shapes for $\beta = \pi$, $b = b' = 0, 5$ and various Weber numbers.

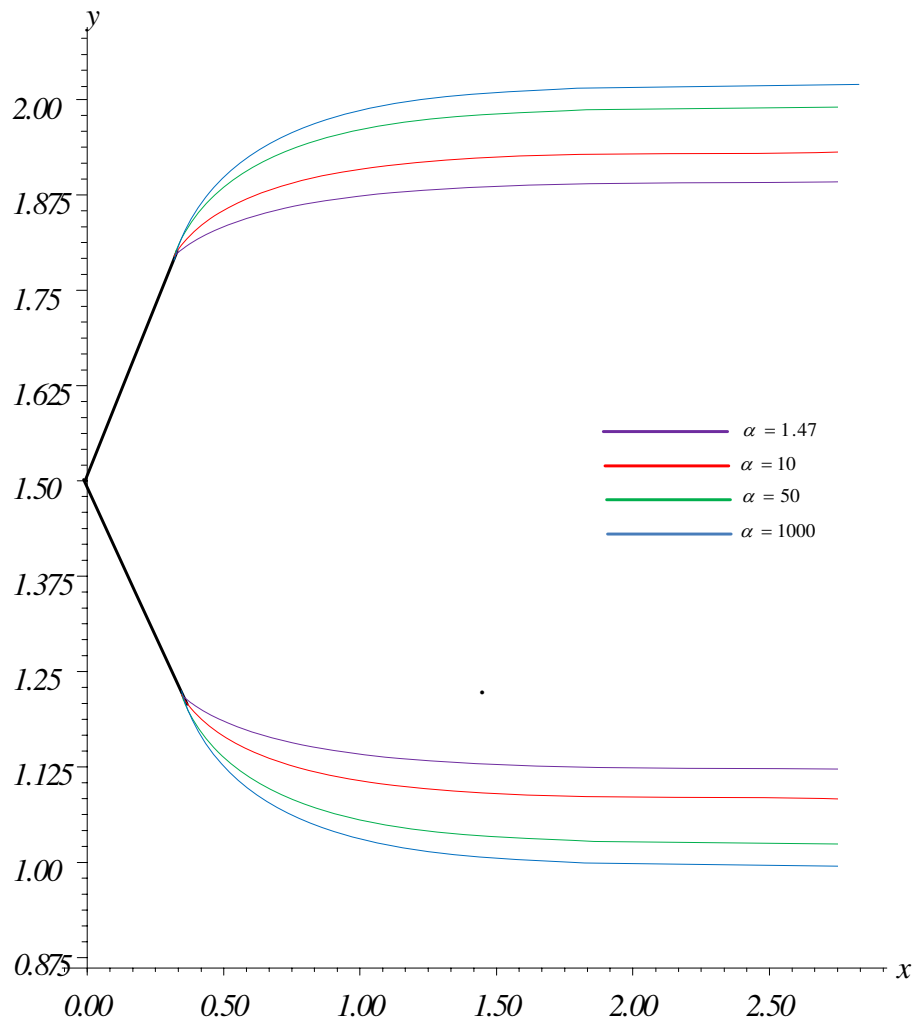


Figure 4.8: Computed free streamline shapes for $\beta = \frac{\pi}{2}$, $b = b' = 0,5$ and various Weber numbers

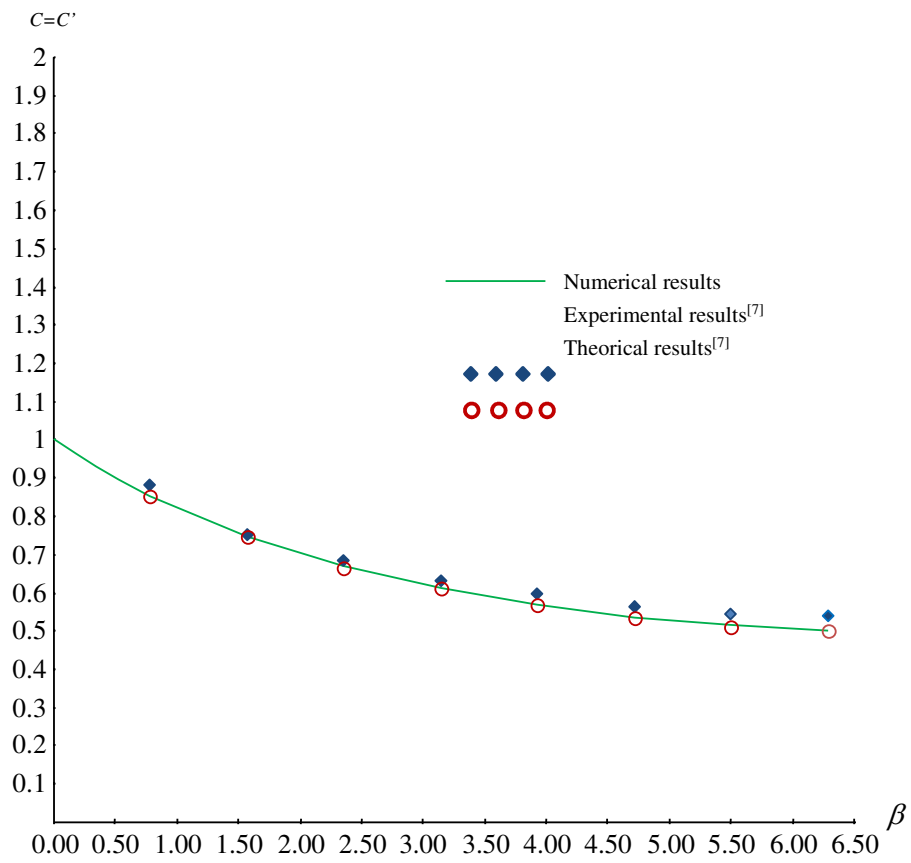


Figure 4.9: Comparison of the obtained results of $C = C'$ for various values of β and $b = b' = 0, 5$ with the experimental and theoretical results given in [7].

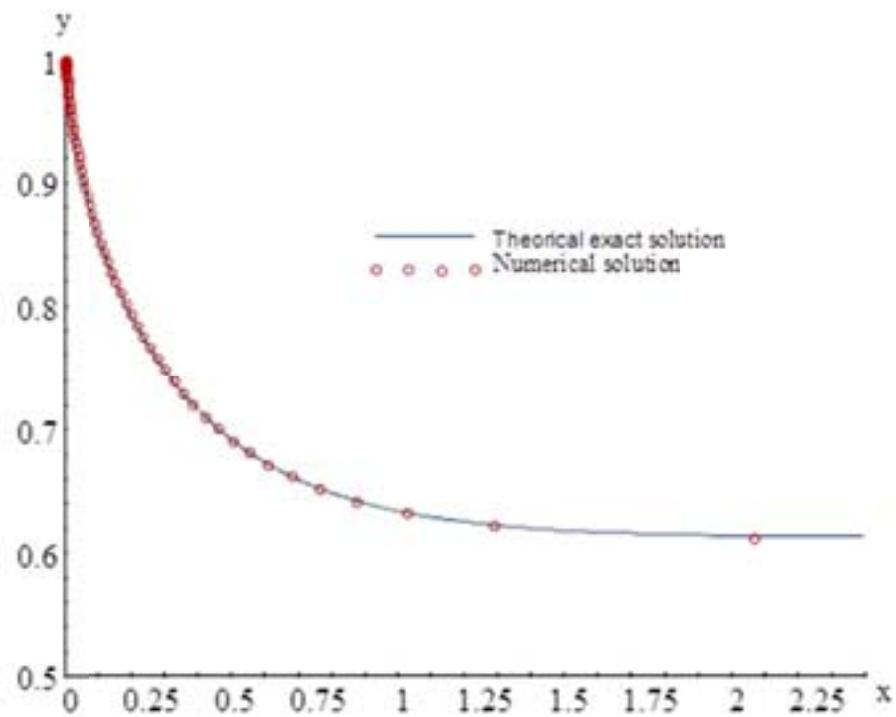


Figure 4.10: Comparison of the calculated free surface with the exact solution for $\beta = \pi$, $b = b' = 1$

general conclusion

In this work, we addressed two problems:

Problem 1: The first problem deals with the influence of an infinite wedge on a very distant jet. We applied the method of hodograph to find exact solutions for the free surface shape in cases where gravity and surface tension are negligible. We found these solutions for the famous wedge angles, which are $\frac{\pi}{6}$, $\frac{\pi}{4}$, $\frac{\pi}{3}$, $\frac{\pi}{2}$, $\frac{2\pi}{3}$, $\frac{3\pi}{4}$, and $\frac{5\pi}{6}$. Subsequently, we numerically solved the problem using the boundary integral equation technique for these wedge angles, taking into account surface tension. This revealed the relative agreement between the numerical and analytical solutions.

Problem 2: The second problem involves the influence of an infinite wedge in a straight tunnel on fluid flow within the channel. We used the method of series truncation to find a solution and the shape of the free surface flow. This technique allows us to precisely determine the type of singularity at the contact point. The resulting solution shows that the effect of surface tension is to reduce the curvature of the free surface. The key advantage of this technique is the reduction in problem dimensionality from two dimensions to one dimension, solving the problem only along the flow domain boundaries.

Bibliography

- [1] Mina B Abd-el Malek and Sarwat N Hanna. Approximate solution of a flow over a ramp for large froude number. *Journal of computational and applied mathematics*, 28:105–117, 1989.
- [2] RC Ackerberg and Ta-Jo Liu. The effects of capillarity on the contraction coefficient of a jet emanating from a slot. *The Physics of fluids*, 30(2):289–296, 1987.
- [3] Abdelkader Amara and Abdelkader Gasmi. The effect of surface tension on the jet flow in u-shaped channel. *International Journal of Pure and Applied Mathematics*, 118(3):625–635, 2018.
- [4] J Asavanant and J-M Vanden-Broeck. Nonlinear free-surface flows emerging from vessels and flows under a sluice gate. *The ANZIAM Journal*, 38(1):63–86, 1996.
- [5] George Keith Batchelor. *An introduction to fluid dynamics*. Cambridge university press, 1967.
- [6] G. Birkhoff and E.H. Zarantonello. *Jets, wakes, and cavities*. Academic Press, 1957.
- [7] Tahar Blizak and Abdelkader Gasmi. Nonlinear free surface flow past a wedge in channel. *INCAS Bulletin*, 15(1):9–19, 2023.
- [8] B Bouderah, A Gasmi, and H Serguine. Zero gravity of free-surface jet flow. In *International Mathematical Forum*, volume 2, pages 3273–3277, 2007.

- [9] May Manal Bounif and Abdelkader Gasmi. First order perturbation approach for the free surface flow over a step with large weber number. *INCAS Bulletin*, 13(2):11–19, 2021.
- [10] Luís Manuel Braga Da Costa Campos. *Complex analysis with applications to flows and fields*. CRC press, 2010.
- [11] MJ Cooker. Potential flow for a steady jet in a wedge. *Quarterly Journal of Mechanics and Applied Mathematics*, 52(1):127–140, 1999.
- [12] GD Crapper. An exact solution for progressive capillary waves of arbitrary amplitude. *Journal of Fluid Mechanics*, 2(6):532–540, 1957.
- [13] M Dormiani, JC Bruch Jr, and JM Sloss. Flow past symmetric convex profiles with open wakes. *International journal for numerical methods in fluids*, 7(12):1301–1314, 1987.
- [14] A Gasmi and H Mekias. The effect of surface tension on the contraction coefficient of a jet. *Journal of Physics A: Mathematical and General*, 36(3):851, 2003.
- [15] Abdelkader Gasmi. Numerical study of two-dimensional jet flow issuing from a funnel. In *Advances in Applied Mathematics*, pages 161–169. Springer, 2014.
- [16] Abdelkader Gasmi. Two-dimensional cavitating flow past an oblique plate in a channel. *Journal of Computational and Applied Mathematics*, 259:828–834, 2014.
- [17] Abdelkader Gasmi and Abdelkader Amara. Free-surface profile of a jet flow in u-shaped channel without gravity effects. *Advanced Studies in Contemporary Mathematics*, 28(3):393–400, 2018.
- [18] Abdelkader Gasmi and Hocine Mekias. A jet from container and flow past a vertical flat plate in a channel with the surface tension effects. *Appl. Math. Sci*, 1(54):2687, 2007.

- [19] Abdelkader Gasmi and Hocine Mekias. A jet from container and flow past a vertical flat plate in a channel with the surface tension effects. *Appl. Math. Sci*, 1(54):2687, 2007.
- [20] MI Gurevich. Theory of jets in ideal fluids. *Translated by RL Street, Stanford University, Academic Press Inc., New York, Printed in the USA, Card Number 65-27087*, 1965.
- [21] J Hureau and R Weber. Impinging free jets of ideal fluid. *Journal of Fluid Mechanics*, 372:357–374, 1998.
- [22] AC King and MIG Bloor. Free-surface flow over a step. *Journal of Fluid Mechanics*, 182:193–208, 1987.
- [23] AC King and MIG Bloor. Free-surface flow of a stream obstructed by an arbitrary bed topography. *The Quarterly Journal of Mechanics and Applied Mathematics*, 43(1):87–106, 1990.
- [24] Abdelkader Laiadi and Abdelkrim Merzougui. Numerical solution of a cavity problem under surface tension effect. *Mathematical Methods in the Applied Sciences*, 44(10):8463–8471, 2021.
- [25] A Merzougui, H Mekias, and F Guechi. Surface tension effect on a two dimensional channel flow against an inclined wall. *Applied Math Sciences*, 1(47):2313–2326, 2007.
- [26] L.M. Milne-Thomson. *Theoretical Hydrodynamics*. Macmillan, 1968.
- [27] PM Naghdi and L Vongsarnpigoon. Steady flow past a sluice gate. *The Physics of fluids*, 29(12):3962–3970, 1986.
- [28] Weidong Peng and David F Parker. An ideal fluid jet impinging on an uneven wall. *Journal of Fluid Mechanics*, 333:231–255, 1997.
- [29] Daniel Edwin Rutherford. *Fluid dynamics*. Oliver and Boyd, 1959.

- [30] YA Semenov and GX Wu. Asymmetric impact between liquid and solid wedges. *Proceedings of the Royal Society A: Mathematical, Physical and Engineering Sciences*, 469(2150):20120203, 2013.
- [31] Bhimsen K Shivamoggi. *Theoretical fluid dynamics*. John Wiley & Sons, 2011.
- [32] AC Smith and TH Lim. Symmetric supercritical free surface flow over a polygonal obstacle. *International journal of engineering science*, 23(3):289–306, 1985.
- [33] Murray R Spiegel. Complex variables: With an introduction to conformal mapping and its applications. (*No Title*), 1964.
- [34] Scott Tooley. *The effects of surface tension on free surface flows intersecting rigid walls*. PhD thesis, University of East Anglia, 2002.
- [35] Jean-Marc Vanden-Broeck. The effect of surface tension on the shape of the kirchhoff jet. *The Physics of fluids*, 27(8):1933–1936, 1984.
- [36] Jean-Marc Vanden-Broeck. Flow under a gate. *The Physics of fluids*, 29(10):3148–3151, 1986.
- [37] Jean-Marc Vanden-Broeck. Cavitating flow of a fluid with surface tension past a circular cylinder. *Physics of Fluids A: Fluid Dynamics*, 3(2):263–266, 1991.
- [38] Jean-Marc Vanden-Broeck. *Gravity-capillary free-surface flows*. Cambridge University Press, 2010.
- [39] R Weber and J Hureau. Ideal fluid flow past obstacles in an arbitrary channel: comparison of numerical and experimental results. *Journal of Fluid Mechanics*, 447:129–148, 2001.
- [40] T Yao-Tsu Wu, Arthur K Whitney, and Christopher Brennen. Cavity-flow wall effects and correction rules. *Journal of Fluid Mechanics*, 49(2):223–256, 1971.